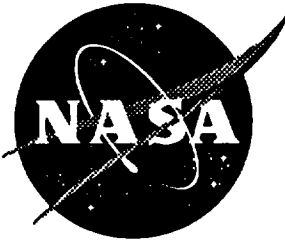


1N-07
24555
P-57



NASA's Hypersonic Research Engine Project - A Review

Earl H. Andrews
Langley Research Center, Hampton, Virginia

Ernest A. Mackley
Analytical Services & Materials, Inc., Hampton, Virginia

(NASA-TM-107759) NASA'S HYPERSONIC
RESEARCH ENGINE PROJECT: A REVIEW
(NASA, Langley Research Center)
57 p

N95-12860

Unclass

G3/07 0027555

October 1994

National Aeronautics and
Space Administration
Langley Research Center
Hampton, Virginia 23681-0001

NASA' S HYPERSONIC RESEARCH ENGINE PROJECT - A REVIEW

by
Earl H. Andrews
NASA Langley Research Center
and
Ernest A. Mackley
Analytical Services and Materials, Inc.
Hampton, VA

SUMMARY

The goals of the NASA Hypersonic Research Engine (HRE) Project, which began in 1964, were to design, develop, and construct a high-performance hypersonic research ramjet/scramjet engine for flight-test over the speed range from Mach 4 to 8 (ref. 1). The project was planned to be accomplished in three phases: project definition, research engine development, and flight test using the X-15A-2 research airplane, which was modified to carry hydrogen fuel for the research engine. The project goal of an engine flight test was lost when the X-15 program was canceled in 1968. Ground tests of full-scale engine models then became the focus of the project with the objectives of determining engine structural/cooling performance and engine internal thrust performance. Two axisymmetric full-scale engine models having an 18-inch-diameter at the cowl leading edge were fabricated: a structural model and a combustion/propulsion model. The models were tested in the NASA Langley 8-Foot High Temperature Structures Tunnel and the NASA Lewis Plum Brook Hypersonic Test Facility, respectively.

A brief historical review of the HRE Project is presented. Tests of the full-scale engine models are described and many associated research/development programs are briefly discussed. Data results from the full-scale engine experimental tests show that both engines performed well. A vast amount of experience was gained from the project, especially during the two engine ground-test programs. To record such experiences, a list of the lessons learned from the overall HRE Project is presented.

INTRODUCTION

For several years prior to 1964, considerable experimental research had been conducted on airbreathing engine inlets and combustor components, as noted in references 2-4. A primary goal of direct-connect combustor tests was to demonstrate the validity of supersonic combustion. The status of this component technology in the early 1960's indicated a high potential for significant advances in hypersonic airbreathing propulsion using a supersonic combustion ramjet (scramjet) engine with hydrogen as both a coolant and the fuel (i.e., a regenerative system). The research results, however, had not been integrated into a complete engine having high performance and operational flexibility over any significant range of speed beyond that obtainable with turbojet engines. NASA's Hypersonic Research Engine Project was formulated in 1964 to meet the need for a program to perform this integration and to accelerate advancement of the technology of airbreathing propulsion for hypersonic atmospheric flight. Langley Research Center was the lead center with the Ames, Dryden, and Lewis Research Centers participating.

The HRE Project's main research objective was to demonstrate high internal thrust performance for a scramjet engine over a Mach number range of 4 to 8; the engine was meant for research and was not in any sense meant to be a prototype of a propulsion system for any particular flight mission. To meet this objective, the HRE Project was planned to be conducted in three phases: project definition in Phase I, research engine development in Phase II, and flight tests using the X-15A-2 research airplane as a test vehicle in Phase III (see fig. 1). In January 1968, during Phase II development, the goal of the project to flight test an engine came to an end

when the X-15 program was canceled. Therefore, ground tests of full-scale engine models became the driving focus of the project. To fulfill the project's redirected goals, two axisymmetric full-scale models with an 18-inch-diameter at the cowl leading edge were constructed. One was a water-cooled, gaseous hydrogen-fueled Aerothermodynamic Integration Model (AIM) that was tested in the NASA Lewis Plum Brook Hypersonic Tunnel Facility at Mach 5, 6, and 7. A second model was of lightweight structure with hydrogen cooling (gaseous H₂ at LN₂ temperatures). This model, the Structures Assembly Model (SAM), was tested in the NASA Langley 8-Foot High-Temperature Structures Tunnel at Mach 7. No combustion in this engine was possible because of an oxygen-deficient tunnel test stream.

A brief historical review is presented herein along with salient features of the HRE Project. Many research/development programs were conducted as part of the HRE Project; these are briefly discussed and some results of the component test programs are included. Results of the AIM and SAM tests are discussed and summarized. Lessons learned from the overall HRE Project are also listed. A large number of contractor documents (NASA contractor reports) and formal NASA reports were generated during the HRE Project; a list of 149 publications is presented in the Appendix.

SYMBOLS

A	area, ft ²
A _{cowl}	cowl area, ft ²
C _S	ratio of actual-to-ideal stream thrust
C _T	internal thrust coefficient, $C_T = \frac{T}{q_\infty A_{cowl}}$
d	fuel injector orifice diameter, in.
I _{sp}	fuel specific impulse, $I_{sp} = \frac{T}{\dot{m}_{fuel}}$, sec
\dot{m}_{cap}	actual captured air mass flow at cowl, lbs/sec
\dot{m}_{cowl}	maximum possible captured air mass flow at cowl, lbs/sec
\dot{m}_{fuel}	fuel flow rate, lbs/sec
M _c	combustor entrance Mach number
M ₀	tunnel nozzle exit Mach number
M _∞	flight Mach number
M _{th}	inlet throat Mach number
p	static pressure, psia
P _{t,0}	tunnel total pressure, psia
P _{t,th}	inlet throat total pressure, psia
q	dynamic pressure, psfa
q _∞	free-stream dynamic pressure, psfa
Q/A	heat transfer rate or load, Btu/ft ² -s
R	radial distance from engine centerline, in
R _C	cowl lip radial distance from engine centerline; vertical tangent point (see Table III), in

RCL	cowl lip radial distance from engine centerline; internal 12° tangent point (see Table III), in
s	circumferential or span-wise spacing between the fuel injector orifices, in.
T	thrust, lbs
T _{fuel}	hydrogen fuel temperature, °R
T _{hot}	heat-exchanger hot surface temperature (see figs. 10 and 11), °R
T _{max}	heat-exchanger hot surface maximum temperature, °R
T _{t,0}	tunnel total temperature, °R
X	longitudinal distance from inlet spike tip (see Table III) or axial length in 2-D combustor model (see figs. 5 (a-c)), in
X _C	longitudinal distance from inlet spike tip to the cowl lip; vertical tangent point (see Table III), in
X _{CL}	longitudinal distance from inlet spike tip to the cowl lip; internal 12° tangent point (see Table III), in
α	angle of attack, degrees
ΔT	temperature change across the hot skin heat -exchanger assembly (see fig. 10), °F
η _c	combustion efficiency
φ	fuel equivalence ratio; φ= 1.0 for stoichiometric combustion
ξ	surface angle with respect to model centerline (see Table III), degrees

Propellants:

CH ₄	gaseous methane
GH ₂ or H ₂	gaseous hydrogen
GN ₂	gaseous nitrogen
GO ₂	gaseous oxygen
LH ₂	liquid hydrogen
LN ₂	liquid nitrogen

Acronyms:

AIM	Aerothermodynamic Integration Model
HRE	Hypersonic Research Engine
HREP	Hypersonic Research Engine Project
HTF	Hypersonic Tunnel Facility
8-Ft. HTST	8-Ft. High-Temperature Structures Tunnel
SAM	Structures Assembly Model
scramjet	supersonic combustion ramjet

PROJECT OBJECTIVE

The HRE Project's main research objective was to demonstrate high internal thrust performance for a ramjet/scramjet engine over a Mach number range of 4 to 8. This task was to be accomplished by means of broad objectives such as: (a) provide focus for application/integration of fundamental and engine component research; (b) generate comparable engine ground and flight test data as a basis for future decisions; (c) guide and stimulate hypersonic airbreathing propulsion research; and (d) establish the validity of existing hypersonic engine research, developmental methods, and future requirements. To meet these broad objectives, the HRE Project was planned to be conducted in three phases: project definition in Phase I, research engine development in Phase II, and flight tests using the X-15A-2 research airplane as a test vehicle in Phase III. The General Electric Company, the Marquardt Corporation, and the AiResearch Manufacturing Company, a division of the Garrett Corporation, participated in the Phase I effort. It is interesting to note that the U.S. Air Force funded further work by the Marquardt Co. and the General Electric Co. on their Phase I HRE concepts. Also, the Air Force funded an effort by the United Aircraft Research Laboratories (now the United Technologies Research Center) with Pratt and Whitney on their proposed Phase I HRE configuration. Results of these Air Force programs are documented in references 5-7. AiResearch was chosen to continue in Phase II of the HRE Program with an axisymmetric configuration. The research value of scramjet flight-test and ground-test data comparison for the selected engine concept was considered to be very high. This concept promised high internal thrust performance but, because of high external drag, would not demonstrate net thrust (internal thrust greater than external drag) above Mach 6. The large drag was a direct result of the HRE Project's goal to flight test the engine on the underside of an X-15 that had a limited supply of hydrogen available for the research engine coolant/fuel. Air flow through the engine was therefore required to be shut off before and after an engine test in flight to conserve hydrogen. The resulting engine inlet geometry achieved this shut-off requirement but at the cost of a high external cowl angle and associated high external drag. This axisymmetric high external drag concept fit well on the X-15 and would fulfill the research goal for good scramjet internal engine performance from X-15 flight tests. The demonstration of net thrust was, therefore, left for future scramjet concepts/tests.

RESEARCH/DEVELOPMENT PROGRAM

Concept

The HRE axisymmetric configuration, figure 2, had a controlled translating spike that could be moved fore and aft from inlet closeoff to full open and to intermediate positions. Inlet closeoff was required to minimize the use of hydrogen coolant before and after the engine test portion of the X-15A-2 flight and to minimize foreign-object damage to the engine during take-off and landing. At the onset of the engine test during the flight, the spike was translated aft from inlet closeoff to allow the inlet to start. The inlet spike was in a fixed position for Mach 4 to 6 operation with the spike-tip shock falling outside of the cowl lip, as shown on the underside of the spike in figure 2. From Mach 6 to 8, the spike-tip shock impinged on the cowl lip, as shown on the top side of the spike in figure 2. This shock-on-lip condition was maintained by translating the spike in a forward direction as the Mach number increased. Subsonic combustion was planned over the Mach range of 4 to 6, with transition from subsonic to supersonic combustion from Mach 5 to 6, and all supersonic combustion up to Mach 8. The locations of the staged fuel injectors, which were used to accomplish these mode changes, are shown in figure 2. The flightweight structure fabrication techniques are also illustrated on the figure.

Various studies which were conducted under the research and development program of the project, including many that were associated with planned X-15 flight experiments, were directed toward the concept shown in figure 2. Progress results and final/terminal reports were extensively documented; many of these documents are listed in the Appendix.

Flight Associated

Development items associated with the flight experiment included fuel systems, a fuel/engine control system, X-15 integration studies, flight instrumentation, and ground support systems for flight tests (refs. 8-13). The fuel system incorporated a turbopump which was a close coupled boot-strapped liquid hydrogen centrifugal hydrogen gas turbine. The turbine utilized the heat energy of the hydrogen cooling, thus eliminating the necessity of an external fuel source. Fuel control valves were also developed during the project to regulate the cold (50° R) and hot (1500° R) hydrogen. Three of the valves regulated the hot hydrogen gas flow to the fuel injectors. A breadboard of the control system was developed, along with the turbopump and valves, as a digital computer software system which embodied a major part of the engine control mechanization. This breadboard system was a fully operational configuration which could be used in simulation studies and wind tunnel testing. No constraints on packaging were imposed, therefore, the breadboard was assembled in a standard 6-ft. rack. The lightweight configuration of this system was designed, however, to be packaged within the nozzle cavity of the engine. The control computer system was designed to receive data from several pressure and temperature sensors in the X-15 flow field, the engine inlet, the fuel manifold, and the engine structure. These data were used to determine commands which were sent to control the inlet geometry by positioning the spike. A computed airflow was used to determine the required fuel flow to the fuel injectors. The control system also regulated the coolant flow to the different structures and if there was an excess amount of coolant (fuel) than was required for burning, this excess fuel would be dumped overboard. The valves and turbopump were developed to the point where they were considered to be prototype flight configuration hardware (fig. 3), but were never used since the X-15 program was canceled prior to any flight tests.

Fabrication/Structures

Fabrication techniques for the cooled structures were developed and partial sections were fabricated. Many tests were performed on sections of the cowl leading edge, the spike tip, the manifold crossovers, and the internal strut. (Several documents of specific structures and cooling development and the structures and cooling interim technical data reports are listed in the Appendix.) Fabrication of defect-free parts was a learning process in that components were made, and remade, until usable or repairable parts were obtained; the success ratio was approximately one out of three.

Inlet Program

An inlet development and test program was conducted in which two different models were tested—a one-third scale model and a two-thirds scale model (refs. 14-16). The one-third scale model was tested at Mach 4 in the Unitary Plan Wind Tunnel at Langley Research Center where inlet starting problems were first encountered. During hot flow tests of the model at Mach 4 in a facility at the Ordnance Aerophysics Laboratory (OAL), Dangerfield, Texas, the model was precooled and the inlet started upon model injection into the tunnel flow but unstarted as the model surface temperature increased. At NASA Langley, the starting problem was studied using actively cooled surfaces to allow the inlet to start and remain started during steady state test conditions (ref. 17). The two-thirds scale inlet model (12-inch-diameter at the inlet cowl leading edge) was then fabricated with active nitrogen (vaporized liquid) cooling and tested at the Arnold Engineering Development Center (AEDC) in tunnels A and B over the Mach number range of 3 to 8.

A photograph of the two-thirds scale model is shown in figure 4(a) along with performance data, pressure recovery and mass flow ratio ($\dot{m}_{cap}/\dot{m}_{cowl}$) versus test Mach number (figs. 4(b) and 4(c), respectively), obtained from the AEDC tests. The performance objectives for these inlet tests are represented by the cross-hatched bands. The test data are represented by the symbols; the triangles are for the subsonic combustion mode and the circles are for the supersonic combustion mode. Inlet spike boundary-layer transition was achieved using various sizes of trip mechanisms that resulted in total-pressure losses. However, the pressure

recoveries all lie within the objective band for the subsonic mode and within or above the objective band for the supersonic mode. The mass flow ratios fell near the objective band.

Combustor Program

A combustor research and development program was conducted at the North American Rockwell (NAR) Thermophysics Laboratory in El Segundo, California. A two-dimensional combustor model, figure 5, was tested that permitted the study of injector size and spacing, staged fuel injection, angled fuel injection, combustor area ratio and wall divergence, and geometry scaling. Combustor entrance air temperature and pressure, fuel temperature, fuel equivalence ratio, fuel ignition and flameholding characteristics, and heat transfer were also investigated (see refs. 18 and 19). A comparison is shown in figure 5(b) of the two-dimensional and AIM combustors configured for Mach 8 free-stream conditions. The 2-D combustor consists of two injector stages, each having two rows of injectors (one each on the top and bottom walls) which were longitudinally spaced as shown in the sketch. The overall 2-D model area ratio and the area ratio between stages closely simulated the AIM engine as shown in the table of figure 5(b). The effect of increased levels of fuel burning (ϕ) on the pressure distribution for the AIM true-scale (0.6- by 6-inch) 2-D test combustor is shown in figure 5(c). The sharp drop in pressure at station 12 was due to divergence of the burner walls. The pressure increases near station 20 were thought to be associated with flow separation. Combustor model scale effect, one of the many effects studied, is shown in figure 5(d) as a comparison of pressure distributions of the 2- by 6-inch and 0.6- by 6 inch (true scale) combustors.

The fuel injector parameters for the two 2-D combustor models were:

Combustor Height, Inch	Hole Diameter, Inch	Hole Spacing, Inch	No. of Holes Bottom/Top
2.0	0.25	1.50	3/3
0.6	0.10	0.55	8/7

Results from the one-dimensional data-analysis program indicated that the peak-flow blockages due to separation were approximately equal for both models (40 percent). However, blockage for the 0.6-inch-high combustor increased much more abruptly from entrance to the peak value, resulting in a higher total pressure loss and an associated higher static pressure, as is evident in figure 5(d), especially for the $\phi = 0.62$ data. Model and facility hardware leakage problems were encountered during the NAR test program that could not be resolved in a timely and economical manner. At the time that the difficulty doing the NAR tests was encountered, the U.S. Air Force had a hydrocarbon-fueled combustor study in progress at the United Aircraft Research Laboratory (UARL) in East Hartford, Connecticut. An agreement between the Air Force and the HRE Project Office allowed additional staged-fuel injection tests with gaseous hydrogen to be performed at the UARL using their two-dimensional model that was modified to closely simulate the AIM configuration (ref. 19). A study of the combustion kinetics was also performed for the diverging combustor to determine the optimum station to inject the hydrogen fuel. Results from both test programs were compared to theoretical analysis and the results were used in the boiler-plate engine (AIM) design (ref. 18).

Nozzle Program

Another subprogram that was conducted during this project was an engine exhaust nozzle research and development program (ref. 20). This program had two major categories—determination of experimental performance and design analysis optimization. Two one-third-scale nozzle models were fabricated and tested (fig. 6); the configuration of one was optimized for Mach 6 conditions and the other for Mach 8 conditions. One nozzle had surface cooling (liquid nitrogen) to allow determination of the overcooling effect upon performance. Direct-connect tests were conducted at the Fluidyne facility in Minneapolis, Minnesota, with an unheated air supply at several incoming Mach numbers; figure 6(b) shows a model configuration installed in the facility. The tests permitted assessment of internal engine centerbody

mounting strut losses, entrance Mach number, plug truncation, initial boundary thickness, and wall cooling effects. The ratio of the actual-to-ideal stream thrust, C_S , was found to be a convenient measure of performance for the HRE nozzle. For one of the nozzle model configurations, the predicted values of C_S are shown in figure 6(c) vs. combustor exit (minimum area between the struts) Mach number. The friction/divergence, strut, and wall cooling predicted losses were based on the experimental results. The minor configuration penalties and the chemical kinetics losses were obtained analytically. A shadowgraph of one of the nozzle tests is shown in figure 6(d).

FLIGHT PROGRAM

The X-15 airplane that was to be used for the HRE flight test was designated the X-15A-2. This aircraft was modified with the addition of a fuselage section to include the hydrogen fuel tank for the HRE. For high-speed flights (Mach 6-8), external drop fuel tanks were attached and used by the X-15A-2 up to about $M = 3.5$ and an ablative thermal protective cover was applied over the entire aircraft.

Aircraft Controllability Flight Tests

Preliminary flights, prior to the actual HRE flight test program, were performed to test the X-15A-2 for controllability with a simulated HRE attached to the underside of the aircraft. The model did not have internal flow passages but did have the external shape of the HRE. Two flight tests were performed with this simulated engine attached, as shown in figure 7. The first flight was conducted at a maximum flight speed of approximately Mach 3.5 without the drop tanks or ablative coating (fig. 7(a)). The second flight was performed at a maximum flight speed of Mach 6.7 on October 3, 1967, with the drop tanks attached and the ablative coating applied (fig. 7(b)); this was the last successful flight of the X-15 program. During this latter flight, structural damage to the aircraft/engine pylon occurred, as a result of shock impingement, to the point that the simulated HRE model fell from the underside of the vehicle on the aircraft's final landing approach.

X-15 Program Cancellation

The X-15 program was very austere in the mid-to-late 1960's, and a decision was made in 1968 to terminate the program. Since the HRE would not be flight tested, the HRE Project focus had to be redirected.

HRE PROJECT REDIRECTION

With the cancellation of the X-15 program, ground tests of full-scale engine models became the driving focus of the HRE Project. The objectives for the project then became: 1) completion of the development of the structural design and validation of the full-scale engine structure by testing of a full-scale hydrogen-cooled structural assembly model of the research engine; and 2) completion of the development of the engine aerothermodynamic design and testing of a full-scale, water-cooled, gaseous hydrogen-fueled aerothermodynamic integration model of the research engine in order to verify engine thrust performance.

STRUCTURES ASSEMBLY MODEL (SAM)

At the time of the X-15 program termination, the HRE Project was conducting a flightweight structures program where engine components (inlet spike, outer shell, etc.) were fabricated and the fabrication processes were evaluated by various destructive and nondestructive testing. A decision was made to assemble the fabricated parts from the flightweight engine structures program, an engine vibration model, and additional required parts into a structural test engine (SAM). This flightweight engine development program had the means to determine system feasibility, establish aerodynamic design methods, design and

fabricate a light-weight cooled structure, and to test the structure in a wind tunnel at conditions simulating Mach 7 flight (refs. 21-23).

Facility and Model

Facility.- The SAM was tested in the NASA Langley 8-Foot High-Temperature Structures Tunnel (HTST) from 1971 to 1972. The facility, shown in figure 8, is a hypersonic blowdown tunnel in which the energy level for simulating hypersonic flight is obtained by burning methane in air in a high pressure combustor (ref. 24). The resulting combustion gases are expanded through a contoured nozzle with an 8-foot exit diameter to obtain a nominal Mach 7 flow in an enclosed 14-foot long open-jet test section. The combustion-heated tunnel flow, not replenished with oxygen (which contained about 4 percent oxygen by volume), was suitable for structural tests but not for combustion tests. A cryogenic hydrogen handling system (fig. 8(b)) was used to provide the cooling medium for the actively cooled model. This system consisted of a gaseous hydrogen supply, a liquid nitrogen bath heat exchanger, flexible lines for transmitting cold hydrogen to and hot hydrogen from the SAM, and vent stacks for dispersing the hydrogen.

Model.- The SAM is shown installed in the HTST in figure 9. The base plate of the mounting strut was flush with the floor of the tunnel, thus allowing the proper alignment of the model in both pitch and yaw. The SAM engine consisted of lightweight structure with all aerodynamic surfaces of brazed, plate-fin sandwich construction with hydrogen cooling as shown in figures 2 and 10. Hasteloy-X (ref. 23) was used in all shells with the hot skin being 0.015-inch thick. Fin density ranged from 16 to 28 per square inch, and fin height varied from 0.020 to 0.153 of an inch as a function of operating temperature, heat fluxes, and geometry requirements. Maximum heat-exchanger hot surface temperature of 2000° R was chosen to satisfy a hot-surface creep-rupture life criterion. The cold structural surface temperature was also limited to maintain a ΔT of about 800° F across the heat exchanger to avoid creep deformations. Thermal fatigue life of the structures used in the SAM was a function of the temperature difference across the structure as determined by the mechanical and thermal test data represented in figure 10. The SAM design was based on the mechanical test data that indicated a fatigue life of approximately 100 cycles at a ΔT of 830° F.

SAM Tests and Results

SAM tests.- Tests of the SAM were conducted at various tunnel flow total pressures and total temperatures as shown in Table I. A run was defined as a blowdown of the wind tunnel in which the model was inserted into the gas stream on the tunnel centerline; during cooling performance tests, a run consisted of a single cycle (model insertion into and withdrawal from the tunnel flow) and during the thermal cycling tests each tunnel run generally consisted of two such cycles (ref. 23). The longest time in the tunnel for any one run occurred at 2200 psia and 3000° R during which the model was in the stream for 116 seconds. At the maximum tunnel conditions, 3300 psia and 3400° R, the run times were 35 to 40 seconds. The average run time at the lower tunnel conditions ($p_{t,0} = 950\text{-}1500$ psia and $T_{t,0} \approx 2700^\circ \text{R}$) was between 50 and 60 seconds. Because of the differences in tunnel total temperatures, the tunnel nozzle exit Mach number varied from 6.3 to 6.8 (due to total pressure losses caused by water vapor condensation).

A series of tests was first conducted at 950 psia and 2600° R, and then proceeded to 1500 psia and 2700° R. This run series was then repeated with hydrogen injection, of course without combustion. A portion of each of these runs was made without injection and followed by H₂ injection to provide data at identical tunnel conditions for direct comparisons with and without fuel injection. After completion of the fuel injection tests, the thermal cycling tests were completed at 1380 psia and 2700° R. The purpose of these latter tests was to accumulate the fatigue damage in the structure. Once these parametric-type runs were completed, the final tests were conducted at the higher pressure and temperature conditions (see Table I).

SAM test results.- Surface temperature distributions on the SAM are presented in figure 11 for steady-state conditions ($p_{t,0} = 3320$ psia and $T_{t,0} = 3400^\circ$ R). The test data are represented by the dashed-line curves and the solid-line curves represent results of an analysis for Mach 8 flight conditions. The steady-state test surface temperatures were generally lower than predicted for the Mach 8 temperatures due to the lower simulated flight Mach number (lower total temperature than for Mach 8) in the experimental tests. Model surface discolorations, figure 12, which are an indicator of high surface temperature, were observed at several locations during post-test inspections after operating with reduced hydrogen coolant flow rates. The coolant flow rates were modulated to obtain the maximum skin surface temperature or the ΔT across the skin of the Mach 8 flight structural design. In all locations, except on the cowl lip, the discoloration patterns were traced to local high heating caused by impinging shock wave patterns, as shown by the dashed lines in figure 12. Local heat transfer rates were estimated for these areas and the associated surface temperatures are represented in figure 11 by the circle symbols. Such discolorations did not occur for runs with the design hydrogen coolant flow rate.

SAM test summary.- A summary of the thermal fatigue data for the SAM tests is shown in Table I. Fifty-five cycles were performed during these tests for a total instream time of 29.7 minutes. During these tests, the measurements of ΔT , surface temperature, and internal cooling passage pressures were used to calculate the combined thermal and mechanical stresses. These calculations were used to estimate the amount by which the engine material elastic limit was exceeded for each thermal cycle. From these results, the total damage fraction was estimated. The 55 test thermal cycles were estimated to amount to a damage fraction of 46 percent (out of a 100-cycle life).

The structural program accomplishments included the development of excellent lightweight hydrogen-cooled structure hardware for the SAM and the partial validation of the structure during ground tests. The results indicated a need for higher design surface temperatures, lower ΔT 's, and a different cooling jacket concept to assure longer engine life with coolant flow rates less than or equal to that required for stoichiometric fuel burning. Some foreign object (debris in the tunnel stream) damage to the cowl leading edge occurred early in the test program. The deformations were sufficiently deep to close some of the 0.020-inch high fin passages and one deformation resulted in a small leak. Numerous other impact damage occurred during subsequent tests, however, none of the damaged areas showed serious signs of distress. Such results indicate that the designed leading edge had considerable tolerance to foreign object impact.

AEROTHERMODYNAMIC INTEGRATION MODEL (AIM)

Prior to the X-15 Program cancellation, a water-cooled boiler-plate engine design and development effort was in progress. During the HRE Project redirection process, the boiler-plate engine was designated the AIM. The AIM was fabricated and delivered to the NASA Lewis Plum Brook Station in August 1971 and prepared for installation in the Hypersonic Tunnel Facility (HTF), figure 13.

Facility and Model

Facility.- The HTF, shown in the photograph of figure 13(a), is an enclosed free-jet blowdown tunnel designed for propulsion testing with true oxygen composition, temperature, and altitude simulation for the Mach number range of 5 to 7 (ref. 25). A pictorial schematic of this facility is shown in figure 13(b) with a cut-away view of the test cabin shown in the top left insert. An induction-heated, drilled-core graphite storage heater was used to heat gaseous nitrogen. Ambient temperature oxygen was then mixed with the heated nitrogen downstream of the heater to produce synthetic air. Diluent nitrogen was also added with the oxygen in the mixer at tunnel operating Mach numbers below 7 to supply the correct temperature and mass flow to the free-jet nozzle. Altitude simulation was accomplished by reducing the flow pressure downstream of the test section with a tunnel diffuser and a single-stage steam ejector exhaust

system. Three interchangeable axisymmetric contoured nozzles (42-inch exit diameters) provided nominal test Mach numbers of 5, 6, and 7. Liquid hydrogen was heated in an induction coil pebble bed heater to 2500° R to ensure that the temperature of the hydrogen gas supplied to the AIM fuel manifolds was at least 1500° R. The operational altitude corridor of the hypersonic research engine is shown in the top right insert of figure 13(b). The cross-hatched region represents the corridor with three different lines shown for constant dynamic pressures. Superimposed on this figure as a dash-line box is the operational capability of the HTF. The AIM tests were performed at Mach numbers of 5, 6, and 7, and are represented by the solid-circle symbols on this insert in figure 13(b). The number of tests and the ranges of test conditions are shown in Table II.

Model.—The AIM is shown installed in the HTF in figure 14—a frontal view looking downstream into the facility diffuser. Engine shroud enclosures were later installed to complete the engine installation.

A schematic, presented in figure 15, illustrates the installation of the AIM in the HTF; engine components are also identified. The AIM was fabricated from nickel 200 with boiler-plate construction and water cooling. It had an 18-inch-diameter at the cowl lip and was approximately 87 inches in length (varied with spike translation). The inlet spike, inner shell, and nozzle plug formed the centerbody and the outerbody consisted of the cowl leading edge, outer shell, and nozzle shroud. The inlet spike was moveable fore and aft and the nozzle plug was fixed. The spike had a 0.125-inch tip radius followed by a 10° half-angle cone, 12° of additional isentropic compression, a 5.645° upsloping (away from the centerline) throat region, and ended with a 9.67-inch radius cylindrical section (see Table III). This spike cylinder moved (with spike movement) over the cylindrical inner shell; the trailing edge of the spike resulted in a 0.264-inch rearward-facing step in a 1.0-inch high or less annular duct (varied with spike movement). More details of the AIM and its flow surface coordinates are documented in references 26-28. The outerbody was connected to the centerbody by six internal struts, which also served as passages for the centerbody fuel and instrumentation. The outer shell was attached to two main mounting struts that were connected to the thrust bed. The thrust bed was suspended from flex plates to allow free movement. The thrust/drag load cell was mounted between the thrust bed and a "hard-point" beam. The engine outer cowl and main mount strut aerodynamic covers were not attached to the engine but to the hard point beam.

Locations of the fuel injectors are also depicted in figure 15. The combustor contained three stages of fuel injectors. The first stage was defined as the region downstream of injectors 1a and 1b; the second, downstream of injectors 2a and 2c; and the third, downstream of injectors 3a and 3b, as shown in figure 15. The first two stages were used for supersonic combustion at the higher flight Mach number simulations and also used to assist in fuel ignition at the lower flight Mach numbers. The third stage was used for subsonic combustion. Table IV lists the parameters of the AIM fuel injectors. For Mach 8 operation, the combustor was designed so that fuel could be injected into the first stage using injectors 1a and 1b up to an equivalence ratio of unity. Inlet spike translation permitted combustion to occur in a constant area section, thereby achieving maximum performance. For supersonic operation below Mach 8, fuel was injected into the combustor in two stages (injector 1a, 1b, and 2a, 2c) in order to prevent thermal choking and inlet unstart. An alternative set of injectors 1c and 4 was provided to add operational flexibility.

There were three sets of ignitors, each set consisting of six equally spaced (peripherally) torch-type hydrogen-oxygen ignitors (see Table IV). The first two sets were used for supersonic combustion. The third set was used for subsonic combustion.

The 0.264-inch step formed at the trailing edge of the spike assembly and the inner shell was used as a flame stabilizer for subsonic combustion during fuel injection from injectors 3a and 3b. The location of the maximum cross-sectional area of the struts formed a geometric throat for subsonic combustion—an area reduction of 5 percent. This throat area was fixed and represented a compromise to provide the best performance for both subsonic and supersonic combustion.

AIM Tests and Results

AIM tests.- The main goal of the AIM tests was to determine internal thrust performance for a complete engine over the Mach number range of 5 to 7 with parametric variation of simulated altitude, angle-of-attack, inlet contraction ratio, and fuel staging. An important engine operational goal was to demonstrate a controlled combustion mode transition from supersonic to subsonic and back to supersonic combustion using staged fuel injection. Inlet-combustor interaction limits, fuel autoignition and H_2/O_2 torch ignition, and combustion mixing length (using exit-flow gas samples, ref. 29) were studied during the AIM tests. Heat-transfer and engine cooling requirements with combustion were also determined from the results of these tests.

AIM inlet performance.- Theoretical performance predictions for the AIM inlet were made (ref. 30) and the AIM inlet test data were analyzed and compared to the predictions (ref. 31). The AIM supersonic inlet total pressure recovery data as a function of inlet throat Mach number was shown in reference 31 to form three distinct trend lines corresponding to the tunnel free-stream Mach numbers, as shown in figure 16. The figure shows the expected result: greater total pressure losses with increased flow compression. The trends include spike position changes (Mach 6 solid symbols), different Reynolds numbers, and 0° and 3° angle-of-attack data.

AIM Combustor pressures.- To understand the flow phenomena inside the combustor, the test data were analyzed one-dimensionally using the equations of momentum, energy, continuity, and state with the reactants and products of combustion in chemical equilibrium. In the combustor, the arithmetic average of the inner and outer wall static pressure distributions were used in the one-dimensional analysis to determine the flow condition and performance. The results of this analysis aided in the understanding of the pressure distributions such as shown in figure 17 and some resultant combustion efficiencies such as represented in figure 18.

Pressure distributions on the combustor cowl inner surface are shown in figure 17 for supersonic and subsonic combustion at Mach 6 with the same equivalence ratio. The combustor entrance Mach number was 2.5 with a total temperature of $3000^\circ R$ and static pressure of 15.6 psia. The bottom curve (circles) shows the pressure distribution without fuel injection. The fluctuation of this curve indicates the presence of strong shock waves downstream of the inlet throat. During Mach 6 tests with the first stage (1a, 1b) only, the fuel-air mixture would not autoignite at Mach 6 even with an equivalence ratio of 0.38. The first stage fuel was ignited either by using the ignitors or by the interaction with the second stage injectors. The top curve (squares) represents the pressure distribution resulting from supersonic combustion (duct flow Mach number determined from data analysis) that occurred when fuel was injected from injectors 1a, 1b, 2a, and 2c. In this case, no interaction between the inlet and the combustor occurred, but strong interaction was observed between the first and second stages. The interaction between the first and second stages considerably enhanced combustion. The pressure disturbance produced by the second stage injection propagated upstream to ignite the first stage and reduced the Mach number between injectors 2a, 2c, to the transonic flow range. In this region, both supersonic and subsonic flow existed and good combustion efficiency (see fig. 18) was achieved. No significant burning was observed in the divergent duct downstream of injector 2a until the internal struts were reached and a pressure increase was observed. In the pressure and temperature range tested, supersonic combustion was difficult to achieve in a divergent duct as previously experienced in the 2-D combustor tests.

The static pressure drop on the inner cowl surface at station 59, downstream of the centerbody 0.264-inch rearward-facing step, may be explained by the expansion waves emanating from the step. The combustion was inhibited locally at the expansion waves and again ignited by the recompression shock. This type of combustion is very similar to a shock-induced combustion process which would cause the recompression shock to assume a steeper angle due to increased backpressures.

During the subsonic combustion mode (triangle-symboled curve of fig. 17), the duct flow Mach number at station 49 was about 2.0. A normal shock at station 49 would have produced a static pressure ratio of about 4.3. However, because of the large combustor throat, sufficient backpressure could not be maintained to support a normal shock. Instead, the flow was diffused through weak shocks to produce the static pressure ratio of about 2 observed in figure 17.

AIM combustor performance.- Combustion efficiency for six different fuel injector combinations are presented in figure 18. As expected, combustion efficiency varied with the injector configuration. Data scatter was observed with the 1a, 1b, 2a, 2c injectors and this injector configuration produced a lower combustion efficiency than the 1b, 2a, 2c configuration.

The sizes and locations of fuel injectors were selected to obtain desired mixing schedules by optimizing the fuel penetration and jet spreading. Combustor design specified that the injectors in each stage to be interdigitated (that is, injector 1a orifices interdigitated with 1b orifices and 2a interdigitated with 2c, etc.) to cover the maximum mixing area in an attempt to increase the mixing efficiency. In the final fabricated configuration, however, the injectors in the first stage (1a, 1b) were positioned inline (see Table IV) and opposed to each other (a fabrication error). The effect of this arrangement was twofold. One effect was the reduced mixing efficiency at higher equivalence ratios where local rich fuel conditions resulted in a lower combustor efficiency. The other effect, which may be more significant, was reduced flow blockage from the first stage in-line injector arrangement.

Examination of the static pressure distributions for different injector combinations revealed that the interaction between the first and second injector stages had significant effects on the overall combustor performance. The shorter longitudinal distance between stages using injectors 1a, 1b, 4, and 2c (see figure 15 and Table IV), or a larger disturbance generated by a single-sided injection from the second stage using injectors 1a, 1b, and 2c, appeared to have enhanced the combustion process. The same interaction between the first and second stages, with most of the fuel in the second stage, gave the best performance, i.e., injector 1b only was used for the first stage and injectors 2a and 2c for the second stage. Fuel injectors 1b, 3a, and 3b were used during the subsonic combustion mode.

AIM internal thrust performance.- Internal thrust performance vs. test Mach number is presented in figure 19 at an equivalence ratio of unity (fuel-air ratio = 0.0293). The Mach 5 data were obtained during subsonic combustion, and the Mach 6 and 7 data were obtained during supersonic combustion. (Mach 7 data were corrected for a test total temperature lower than flight simulation (see ref. 23). The cross-hatched bands in figure 19 represent the internal performance levels of ramjet/scramjets. Points on the upper line of the bands are considered to be obtainable only by engines optimized for the Mach number of that point. The lower line of the bands represents the HRE internal thrust performance goals.

The test data were obtained for a water-cooled engine, whereas performance goals were based on a regeneratively cooled system. Since the AIM was water-cooled, wall temperatures in the combustor were much lower than for a comparable hydrogen-cooled flight engine. To obtain a realistic comparison of test data (open-circle symbols) with test goals, the thrust coefficient and specific impulse were corrected to that of a regeneratively cooled system (filled-circle symbols). Caution was exercised for large temperature variations because the correction correlation was not accurate if a change in the combustion process had occurred. Essentially, the correction involved calculating combustor exit conditions at the same enthalpy as a regenerative system and at the given test total pressure and combustor efficiency, then expanding the flow to the nozzle exit to determine gross thrust for a regeneratively cooled system. The correction to Mach 5 data was relatively small (about 2 percent), while at Mach 7 it was relatively large (about 12 percent). Close agreement between corrected performances and the HRE goals is evident in figure 19.

Analyses of the test data indicated that the AIM nozzle performance was about 3 to 4 percent lower than expected relative to the 1/3-scale nozzle model tests. Estimates for internal thrust and impulse that would have been attained had the nozzle performance been the same as measured in the 1/3-scale nozzle model tests are shown as the triangle symbols which are above the HRE performance goals in figure 19. These differences in performance were postulated to be related to the turbulence energy generated by the combustion processes and not recovered in the AIM nozzle.

AIM test summary.- A summary of the AIM tests is presented in Table II. Facility/engine checkout tests were performed from September 1972 through May 1973. During this time, the tunnel/model shrouding was modified to yield good tunnel operations (ref. 26). The first complete fuel-burning test was conducted at Mach 6 conditions on October 5, 1973. A majority of the tests were performed at the Mach 6 conditions (see Table II). Some tests were conducted at different total pressures than the nominal value to determine the effect of altitude (dynamic pressure) on engine performance. Pressure (altitude) had a significant effect on combustor efficiency and overall performance. In the range of pressures tested, the ignition delay reversal effect could occur. The best engine performance corresponded to the combustor entrance pressure that could produce the minimum ignition delay time. One test was performed at an angle of attack of 3° for each of the three Mach numbers.

A total of 52 complete tests were conducted for a total test time (steady-state conditions) of almost 112 minutes. Some model hardware difficulties were encountered, mainly during the initial tests. During the tests when the facility flow was not completely started (i.e., test cabin pressure was greater than the facility nozzle exit pressure), shocks were produced that impinged upon the model. As a result, some areas on the cowl were overheated, with associated thermal expansion, that sheared several bolts/rivets. Also, some binding of the engine metric and non-metric hardware was detected. The binding was attributed to the fact that the engine assembly was performed with the two mounting struts supporting the engine as legs, and the model was then suspended from the struts (inverted position) in the tunnel installation. This binding was corrected prior to resumption of tests in the fall of 1973. Another problem detected during initial checkout testing resulted from having to purge with gaseous nitrogen the internal cavity created between the outer cowl and the outer shell (see fig. 15). The cavity dimension and bleed gaps varied with model heating that made it difficult to determine a true tare force associated with the cavity purging.

The AIM program was a major accomplishment of testing a complete (inlet, combustor, and nozzle), large-scale engine to demonstrate high internal thrust performance for a scramjet/ramjet engine over a Mach number range. Maximum internal thrust performance of the AIM met the HRE internal thrust performance goals. An unexpected result was observed for staged fuel injection. A strong stage interaction occurred and the second stage combustion efficiency was reduced, as deduced from the one-dimensional analysis of the data, by oxygen depletion near the wall. The fuel-air ratio effect was very similar to the predicted values. Performance degradation of about 15 percent was noted at 3° angle of attack. The effects of variations in the inlet contraction ratio were also determined. Stable inlet operation was observed during all tests; inlet unstarts were determined for various fuel injection locations. Single-stage mixing lengths were the same as predicted (ref. 27). Fuel autoignition and use of fuel ignitors were successfully demonstrated. An important result was the demonstration of a smooth transition from a supersonic to subsonic mode of combustion. The supersonic-to-transonic transition region showed a significant static pressure rise which moved upstream as fuel flow was increased, eventually causing inlet unstart. Measured heat loads to the various components of the AIM indicated that the engine overall heat transfer was very close to predictions. Details of the AIM tests and analyses are contained in references 26 through 28.

CONCLUSIONS

Remarks

The original Hypersonic Research Engine (HRE) Project objectives included the necessary research, the engine design, the fabrication, and the ground and flight testing of a ramjet/scramjet engine. The flight test performance objective was eliminated when the X-15 Program was canceled. However, the level of ramjet/scramjet technology was greatly improved by the HRE Project ground test program.

Measured scramjet engine structural performance was obtained using a hydrogen-cooled, lightweight Structures Assembly Model (SAM) engine in tests in the NASA Langley 8-Foot High-Temperature Structures Tunnel (HTST) at a Mach number of 7. Surface pressures, temperatures, and heat fluxes were measured throughout the engine. Predicted surface temperatures representative of those at flight conditions were obtained by undercooling the surfaces; predicted flight-like structural temperature differences, also representative of those at flight conditions (hot surface temperature minus coolant-side surface temperature) were obtained by overcooling the engine structure. Using this technique, the thermal stresses expected in flight were duplicated during the tunnel testing. The combustor and nozzle heat fluxes expected in flight could not be duplicated because of an oxygen-deficient test stream (4 percent by volume) in the 8-Ft. HTST. Since there was no combustion within the engine, the internal engine maximum heat fluxes were only 40 percent of expected flight values. Approximately 46 percent of the predicted thermal fatigue life of the SAM (100 cycles) was used during the 55 test thermal cycles. No problems with the cooling or cooling control systems were found. Tunnel debris caused a few perforations in the hydrogen-cooled leading edge of the SAM cowl. This damage caused no distress to the cooling system or problems to the leading edge or internal cooling jackets.

Ramjet/scramjet internal thrust performance was determined from measurements obtained in ground tests using an 18-inch diameter (at cowl lip), water-cooled, boiler-plate, hydrogen-burning Aerothermo-dynamic Integration Model (AIM). These tests were conducted in the NASA Lewis Plum Brook Station Hypersonic Test Facility at Mach numbers of 5, 6, and 7. The Mach 5 and 6 test conditions were full simulation (total pressure and total temperature) of flight conditions. The Mach 7 condition was limited to a total temperature of about 3200° R because of facility limitations. Engine performance was corrected for the free-stream temperature variations. Caution was exercised for large temperature variations because the correction correlation was not accurate if a change in the combustion process had occurred. Good ramjet/scramjet engine performance was obtained over the Mach number range tested. Engine wall temperatures were much colder in the combustor and nozzle for the water-cooled engine than would be expected for flight; therefore, an energy balance process was used to correct the measured engine performance values which met the HRE internal thrust performance goals.

Lessons Learned

Some of the lessons learned during the HRE Project are briefly stated below for future use (also see ref. 32):

1. Free-jet engine tests with high blockage engine models should be preceded by small-scale model tests to explore tunnel starting and engine/facility interaction.
2. Purging the internal cavities of an engine being used for thrust measurements should be done with care to avoid unwanted tare forces.
3. Thrust measuring models should be fabrication assembled in a manner similar to the tunnel installation configuration to avoid binding problems between metric and non-metric parts. (That is, if the model is to be suspended, then the model fabrication assembly should be performed using a "hanging" assembly rig.)

4. Tunnel starting loads analyses are usually performed considering the pressure loads only. Thermal loads should also be considered to avoid bolt/rievet shearing that may occur because of peak thermal loads.

5. Correcting measured engine thrust values to flight requires sufficient ground measurements and flight analyses to make the correct energy balance.

6. Inlet boundary layer transition is difficult to achieve artificially and causes a large total-pressure loss at hypersonic speeds. Transition occurs naturally in high adverse pressure gradient regions and corresponds to the highest total-pressure recovery; i.e., total pressure loses less with natural than with artificial transition.

7. Combustion mode transition, i.e., subsonic to supersonic or the reverse, was relatively easy to achieve by switching the fuel injection locations, and thus heat distribution, in the HRE diverging combustor with the presence of a 5-percent local area reduction at the aft end of the combustor (a result of the location of internal struts).

8. The effect of inlet flow on combustor performance and combustor flow on nozzle performance was very pronounced in the fuel-burning engine tests (AIM). Therefore, engine performance obtained from integration of results from individual component tests should be used with caution.

APPENDIX

Bibliography

Published Reports From the Langley Hypersonic Research Engine Project Office (HREP)

The reports listed are available from:

NASA—Center for Aerospace Information
P.O. Box 8757
Baltimore, MD 21240
(301) 621-0100
(410) 859-5300
(301) 621-0134 (Fax)

1. *HREP—Diffusion Controlled Combustion for Scramjet Application—Part I—Analysis and Results of Calculations.* General Applied Sciences Laboratories Rep. 569, Dec. 1965. (Available as NASA CR-66363.)
2. *HREP—Diffusion Controlled Combustion for Scramjet Application—Part II—Programmers Manual.* General Applied Sciences Laboratories Rep. 569, Dec. 1965. (Available as NASA CR-66714.)
3. *HREP—Conceptual and Preliminary Design of the Hypersonic Ramjet—Conceptual Study Report.* G.E. Rep. R66FPD69, Feb. 28, 1966. (Available as NASA CR-66219.)
4. *HREP—Conceptual and Preliminary Design of the Hypersonic Ramjet—Conceptual Study Report.* G.E. Rep. R66FPD70, Feb. 28, 1966. (Available as NASA CR-66220.)
5. *HREP—Phase I—Conceptual Design Study Report—Volume I.* AiResearch Rep. AP-66-0167-1, Feb. 28, 1966. (Available as NASA CR-66221.)
6. *HREP—Phase I—Conceptual Design Study Report—Volume II—Appendix A.* AiResearch Rep. AP-66-0167-2, Feb. 28, 1966. (Available as NASA CR-66222.)
7. *HREP—Phase I—Conceptual Design Study Report—Volume III—Appendix B.* AiResearch Rep. AP-66-0167-3, Feb. 28, 1966. (Available as NASA CR-66223.)
8. *HREP—Phase I—Preliminary Design Report—Volume I.* AiResearch Rep. AP-66-0168-1, Feb. 28, 1966. (Available as NASA CR-66224.)
9. *HREP—Phase I—Preliminary Design Report—Volume II—Appendix A.* AiResearch Rep. AP-66-0168-2, Feb. 28, 1966. (Available as NASA CR-66225.)
10. *HREP—Phase I—Preliminary Design Report—Volume III—Appendix B.* AiResearch Rep. AP-66-0168-3, Feb. 28, 1966. (Available as NASA CR-66226.)
11. *HREP—Phase I—Preliminary Design Drawings—Preliminary Design Report—Volume IV—Appendix C.* AiResearch Rep. AP-66-0168-4, Feb. 28, 1966. (Available as NASA CR-66227.)
12. *HREP—Conceptual Design Report—Volume I—Analysis.* Marquardt Rep. 6101, Feb. 28, 1966. (Available as NASA CR-66228.)
13. *HREP—Conceptual Design Study Report—Volume II—Appendices.* Marquardt Rep. 6101, Feb. 28, 1966. (Available as NASA CR-66229.)
14. *HREP—Preliminary Design Report—Volume I—MA-165 Design Description.* Marquardt Rep. 6102, Feb. 28, 1966. (Available as NASA CR-66230.)
15. *HREP—Preliminary Design Report—Volume II—Appendices.* Marquardt Rep. 6102, Feb. 28, 1966. (Available as NASA CR-66231.)

APPENDIX
(continued)

16. *HREP—Phase IIA—Phase I Boilerplate Engine Tests.* AiResearch Rep. AP-67-2536 (Data Item 55-12.01), Aug. 18, 1967. (Available as NASA CR-66777.)
17. *HREP—Phase IIA—Inlet Program, Fourth Interim Technical Data Report.* AiResearch Rep. AP-68-3431 (Data Item 55-1.04), Mar. 29, 1968. (Available as NASA CR-66778.)
18. *HREP—Phase IIA—Inlet Program, Third Interim Technical Data Report.* AiResearch Rep. AP-67-3021 (Data Item 55-1.03), Dec. 13, 1967. (Available as NASA CR-66779.)
19. *HREP—Phase IIA—Inlet Program, Fifth Interim Technical Data Report.* AiResearch Rep. AP-68-3872 (Data Item 55-1.05), June 25, 1968. (Available as NASA CR-66780.)
20. *HREP—Phase IIA—Inlet Program, Seventh Interim Technical Data Report.* AiResearch Rep. AP-68-4656 (Data Item 55-1.07), Jan. 7, 1969. (Available as NASA CR-66781.)
21. *HREP—Phase IIA—Inlet Program, Second Interim Technical Data Report.* AiResearch Rep. AP-67-2582 (Data Item 55-1.02), Sept. 25, 1967. (Available as NASA CR-66782.)
22. *HREP—Phase IIA—Inlet Program, First Interim Technical Data Report.* AiResearch Rep. AP-67-2202 (Data Item 55-1.01), June 9, 1967. (Available as NASA CR-66783.)
23. *HREP—Phase IIA—Inlet Program, Sixth Interim Technical Data Report.* AiResearch Rep. AP-68-4274 (Data Item 55-1.06), Sept. 26, 1968. (Available as NASA CR-66784.)
24. *HREP—Phase IIA—Inlet Program, Terminal Summary Report.* AiResearch Rep. AP-69-4883 (Data Item 55-1.08), Mar. 27, 1969. (Available as NASA CR-66797.)
25. *HREP—Phase IIA—Test Report on Fatigue Testing of Nickel-200 Panels.* AiResearch Rep. AP-68-4617, Jan. 10, 1969. (Available as NASA CR-66842.)
26. *HREP—Phase IIA—Experimental Investigation of the Cooling and Structural Performance for the HRE Cowl Leading Edge.* AiResearch Rep. AP-69-5347 (Data Item 63.01), July 30, 1969. (Available as NASA CR-66843.)
27. *HREP—Phase IIA—Category I Test Report on Passage Fin Heat Transfer and Pressure Drop.* AiResearch Rep. AP-69-5348 (Data Item 63.02), Aug. 7, 1969. (Available as NASA CR-66844.)
28. *HREP—Phase IIA—Braze Alloy Investigation and Flat Panel Testing.* AiResearch Rep. AP-68-3813, May 27, 1968. (Available as NASA CR-66845.)
29. *HREP—Phase IIA—Hastelloy-X Annealing and Chemical Milling Evaluation.* AiResearch Rep. AP-68-3989, July 11, 1968. (Available as NASA CR-66910.)
30. *HREP—Phase II—The Development of a 5-Inch Diameter Vitiation Heater.* AiResearch Rep. AP-70-6047 (Data Item 54.08), Feb. 16, 1970. (Available as NASA CR-66927.)
31. *HREP—Phase II—Combustor Program, Final Technical Data Report.* AiResearch Rep. AP-70-6054 (Data Item 55-2.11), Mar. 23, 1970. (Available as NASA CR-66932.)
32. *HREP—Phase II—Category I Test Report on Structural Thermal Performance and Thermal Cycle Testing.* AiResearch Rep. AP-69-5547 (Data Item 63.04), Oct. 3, 1969. (Available as NASA CR-66943.)
33. *HREP—Phase II—Chemical Kinetics Study for a Supersonic Combustor Model.* AiResearch Rep. AP-70-6319 (Data Item 54.10), May 20, 1970. (Available as NASA CR-66952.)
34. *HREP—Phase IIA—Combustor Program, First Interim Technical Data Report.* AiResearch Rep. AP-67-2162 (Data Item 55-2.01), May 12, 1967. (Available as NASA CR-66955.)
35. *HREP—Phase IIA—Combustor Program, Second Interim Technical Data Report.* AiResearch Rep. AP-67-2535 (Data Item 55-2.02), Sept. 1, 1967. (Available as NASA CR-66956.)

APPENDIX
(continued)

36. *HREP—Phase IIA—Combustor Program, Third Interim Technical Data Report.* AiResearch Rep. AP-67-2832 (Data Item 55-2.03), Dec. 4, 1967. (Available as NASA CR-66957.)
37. *HREP—Phase IIA—Combustor Program, Fourth Interim Technical Data Report.* AiResearch Rep. AP-67-3134 (Data Item 55-2.04), Feb. 19, 1968. (Available as NASA CR-66958.)
38. *HREP—Phase IIA—Combustor Program, Fifth Interim Technical Data Report.* AiResearch Rep. AP-68-3753 (Data Item 55-2.05), May 31, 1968. (Available as NASA CR-66959.)
39. *HREP—Phase IIA—Combustor Program, Sixth Interim Technical Data Report.* AiResearch Rep. AP-68-4128 (Data Item 55-2.06), Aug. 6, 1968. (Available as NASA CR-66960.)
40. *HREP—Phase IIA—Combustor Program, Seventh Interim Technical Data Report.* AiResearch Rep. AP-68-4439 (Data Item 55-2.07), Nov. 18, 1968. (Available as NASA CR-66961.)
41. *HREP—Phase IIA—Combustor Program, Eighth Interim Technical Data Report.* AiResearch Rep. AP-69-4710 (Data Item 55-2.08), Mar. 6, 1969. (Available as NASA CR-66962.)
42. *HREP—Phase IIA—Combustor Program, Ninth Interim Technical Data Report.* AiResearch Rep. AP-69-5038 (Data Item 55-2.09), May 16, 1969. (Available as NASA CR-66963.)
43. *HREP—Phase IIA—Combustor Program, Tenth Interim Technical Data Report.* AiResearch Rep. AP-69-5405 (Data Item 55-2.10), Aug. 21, 1969. (Available as NASA CR-66964.)
44. *HREP—Phase II—Structures and Cooling Development, Thirteenth Interim Technical Data Report.* AiResearch Rep. AP-70-6202 (Data Item 55-7.13), May 27, 1970. (Available as NASA CR-66982.)
45. *HREP—Phase II—Structures and Cooling Development, Twelfth Interim Technical Data Report.* AiResearch Rep. AP-70-6116 (Data Item 55-7.12), Mar. 11, 1970. (Available as NASA CR-66983.)
46. *HREP—Phase II—Aerothermodynamic Integration Model Development, Eighth Interim Technical Data Report.* AiResearch Rep. AP-70-6397 (Data Item 55-4.08), Apr. 24, 1970. (Available as NASA CR-66984.)
47. *HREP—Phase II—Aerothermodynamic Integration Model Development, Seventh Interim Technical Data Report.* AiResearch Rep. AP-69-5899 (Data Item 55-4.07), Jan. 16, 1970. (Available as NASA CR-66985.)
48. *HREP—Phase IIA—Structures and Cooling Development, Fourth Interim Technical Data Report.* AiResearch Rep. AP-68-3250 (Data Item 55-7.04), Mar. 1, 1968. (Available as NASA CR-66986.)
49. *HREP—Phase IIA—Structures and Cooling Development, Fifth Interim Technical Data Report.* AiResearch Rep. AP-68-3754 (Data Item 55-7.05), May 24, 1968. (Available as NASA CR-66987.)
50. *HREP—Phase IIA—Boilerplate Engine Development, First Interim Technical Data Report.* AiResearch Rep. AP-68-3895 (Data Item 55-4.01), July 9, 1968. (Available as NASA CR-66988.)
51. *HREP—Phase IIA—Boilerplate Engine Development, Second Interim Technical Data Report.* AiResearch Rep. AP-68-4285 (Data Item 55-4.02), Oct. 11, 1968. (Available as NASA CR-66989.)
52. *HREP—Phase IIA—Boilerplate Engine Development, Third Interim Technical Data Report.* AiResearch Rep. AP-69-4674 (Data Item 55-4.03), Jan. 24, 1969. (Available as NASA CR-66990.)
53. *HREP—Phase IIA—Aerothermodynamic Integration Model Development, Fifth Interim Technical Data Report.* AiResearch Rep. AP-69-5298 (Data Item 55-4.05), July 8, 1969. (Available as NASA CR-66991.)
54. *HREP—Phase IIA—Aerothermodynamic Integration Model Development, Sixth Interim Technical Data Report.* AiResearch Rep. AP-69-5572 (Data Item 55-4.06), Oct. 14, 1969. (Available as NASA CR-66992.)
55. *HREP—Phase IIA—Aerothermodynamic Integration Model Development, Fourth Interim Technical Data Report.* AiResearch Rep. AP-69-4932 (Data Item 55-4.04), Apr. 15, 1969. (Available as NASA CR-66993.)
56. *HREP—Phase IIA—Structures and Cooling Development, Sixth Interim Technical Data Report.* AiResearch Rep. AP-68-4173 (Data Item 55-7.06), Aug. 31, 1968. (Available as NASA CR-66994.)

APPENDIX
(continued)

57. *HREP—Phase IIA—Structures and Cooling Development, Seventh Interim Technical Data Report.* AiResearch Rep. AP-68-4482 (Data Item 55-7.07), Nov. 27, 1968. (Available as NASA CR-66995.)
58. *HREP—Phase IIA—Structures and Cooling Development, Third Interim Technical Data Report.* AiResearch Rep. AP-67-2833 (Data Item 55-7.03), Dec. 4, 1967. (Available as NASA CR-66996.)
59. *HREP—Phase IIA—Structures and Cooling Development, First Interim Technical Data Report.* AiResearch Rep. AP-67-2161 (Data Item 55-7.01), May 12, 1967. (Available as NASA CR-66997.)
60. *HREP—Phase IIA—Structures and Cooling Development, Eighth Interim Technical Data Report.* AiResearch Rep. AP-69-4759 (Data Item 55-7.08), Feb. 27, 1969. (Available as NASA CR-66998.)
61. *HREP—Phase IIA—Structures and Cooling Development, Ninth Interim Technical Data Report.* AiResearch Rep. AP-69-5075 (Data Item 55-7.09), Jun. 3, 1969. (Available as NASA CR-66999.)
62. *HREP—Phase IIA—Nozzle, Terminal Summary Report.* AiResearch Rep. AP-68-4451 (Data Item 55-3.05), Dec. 17, 1968. (Available as NASA CR-101532.)
63. *HREP—Phase IIA—Structures and Cooling Development, Tenth Interim Technical Data Report.* AiResearch Rep. AP-69-5390 (Data Item 55-7.10), Aug. 26, 1969. (Available as NASA CR-111769.)
64. *HREP—Phase IIA—Structures and Cooling Development, Second Interim Technical Data Report.* AiResearch Rep. AP-67-2537 (Data Item 55-7.02), Aug. 23, 1967. (Available as NASA CR-111770.)
65. *HREP—Phase IIA—Fuel System Development, Third Interim Technical Data Report.* AiResearch Rep. AP-67-3130 (Data Item 55-5.03), Jan. 11, 1968. (Available as NASA CR-111893.)
66. *HREP—Phase IIA—Control System Development, Third Interim Technical Data Report.* AiResearch Rep. AP-67-3131 (Data Item 55-6.03), Feb. 2, 1968. (Available as NASA CR-111894.)
67. *HREP—Phase IIA—Fuel System Development, Fourth Interim Technical Data Report.* AiResearch Rep. AP-68-3588 (Data Item 55-5.04), May 6, 1968. (Available as NASA CR-111895.)
68. *HREP—Phase IIA—Control System Development, Fourth Interim Technical Data Report.* AiResearch Rep. AP-68-3589 (Data Item 55-6.04), May 22, 1968. (Available as NASA CR-111896.)
69. *HREP—Phase IIA—Fuel System Development, First Interim Technical Data Report.* AiResearch Rep. AP-67-2386 (Data Item 55-5.01), Jun. 30, 1967. (Available as NASA CR-111897.)
70. *HREP—Phase IIA—Fuel System Development, Fifth Interim Technical Data Report.* AiResearch Rep. AP-68-3995 (Data Item 55-5.05), Aug. 22, 1968. (Available as NASA CR-111898.)
71. *HREP—Phase IIA—Fuel System Development, Second Interim Technical Data Report.* AiResearch Rep. AP-67-2693 (Data Item 55-5.02), Oct. 18, 1967. (Available as NASA CR-111899.)
72. *HREP—Phase IIA—Fuel System Turbopump Development, Terminal Summary Report.* AiResearch Rep. AP-68-4472 (Data Item 55-5.07), Nov. 4, 1968. (Available as NASA CR-111900.)
73. *HREP—Phase IIA—Fuel System Development (Components), Sixth Interim Technical Data Report.* AiResearch Rep. AP-68-4429 (Data Item 55-5.06), Nov. 1, 1968. (Available as NASA CR-111901.)
74. *HREP—Phase IIA—Fuel System Development, Terminal Summary Report.* AiResearch Rep. AP-68-4611 (Data Item 55-5.08), Dec. 17, 1968. (Available as NASA CR-111902.)
75. *HREP—Phase IIA—Fuel System Development, Terminal Summary Report.* AiResearch Rep. AP-68-4540 (Data Item 55-6.06), Apr. 16, 1969. (Available as NASA CR-111903.)
76. *HREP—Phase II—Metal Joining Efforts Performed in Conjunction with the AIM Development Program.* AiResearch Rep. AP-71-7091 (Data Item 54.13), Feb. 8, 1971. (Available as NASA CR-111904.)

APPENDIX
(continued)

77. *HREP—Phase IIA—Control System Development, First Interim Technical Data Report.* AiResearch Rep. AP-67-2467 (Data Item 55-6.01), Jul. 27, 1967. (Available as NASA CR-111914.)
78. *HREP—Phase IIA—Control System Development, Fifth Interim Technical Data Report.* AiResearch Rep. AP-68-4129 (Data Item 55-6.05), Aug. 27, 1968. (Available as NASA CR-111915.)
79. *HREP—Phase IIA—Control System Development, Second Interim Technical Data Report.* AiResearch Rep. AP-67-2694 (Data Item 55-6.02), Oct. 30, 1967. (Available as NASA CR-111927.)
80. *HREP—Phase II—Structures Assembly Model Test Report Data.* AiResearch Rep. AP-71-7702 (Data Item 63.05), Sept. 22, 1971. (Available as NASA CR-111993.)
81. *HREP—Phase II—Structures and Cooling Development, Fourteenth Interim Technical Data Report.* AiResearch Rep. AP-70-6640 (Data Item 55-7.14), Sept. 1, 1970. (Available as NASA CR-112055.)
82. *HREP—Phase II—Structures and Cooling Development, Fifteenth Interim Technical Data Report.* AiResearch Rep. AP-70-6939 (Data Item 55-7.15), Nov. 24, 1970. (Available as NASA CR-112056.)
83. *HREP—Phase II—Structures and Cooling Development, Sixteenth Interim Technical Data Report.* AiResearch Rep. AP-71-7185 (Data Item 55-7.16), Mar. 18, 1971. (Available as NASA CR-112057.)
84. *HREP—Phase II—Aerothermodynamic Integration Model Development, Tenth Interim Technical Data Report.* AiResearch Rep. AP-70-6800 (Data Item 55-4.10), Oct. 15, 1970. (Available as NASA CR-112058.)
85. *HREP—Phase II—Aerothermodynamic Integration Model Development, Eleventh Interim Technical Data Report.* AiResearch Rep. AP-70-7035 (Data Item 55-4.11), Jan. 6, 1971. (Available as NASA CR-112059.)
86. *HREP—Phase II—Aerothermodynamic Integration Model Development, Twelfth Interim Technical Data Report.* AiResearch Rep. AP-71-7279 (Data Item 55-4.12), Mar. 30, 1971. (Available as NASA CR-112060.)
87. *HREP—Phase II—Structures and Cooling Development, Final Technical Data Report.* AiResearch Rep. AP-72-8237 (Data Item 55-7.18), May 18, 1972. (Available as NASA CR-112087.)
88. *HREP—Phase IIA—X15A-2 Integration Program, Third Interim Technical Data Report.* AiResearch Rep. AP-68-3426 (Data Item 55-9.03), Mar. 11, 1968. (Available as NASA CR-112275.)
89. *HREP—Phase IIA—Ground Support Equipment Development, Terminal Summary Report.* AiResearch Rep. AP-68-4301 (Data Item 55-10.05), Sept. 26, 1968. (Available as NASA CR-112276.)
90. *HREP—Phase IIA—X15A-2 Integration Program, Second Interim Technical Data Report.* AiResearch Rep. AP-67-2834 (Data Item 55-9.02), Nov. 22, 1967. (Available as NASA CR-112277.)
91. *HREP—Phase IIA—X15A-2 Integration Program, First Interim Technical Data Report.* AiResearch Rep. AP-67-2538 (Data Item 55-9.01), Aug. 31, 1967. (Available as NASA CR-112278.)
92. *HREP—Phase IIA—Ground Support Equipment Development, Second Interim Technical Data Report.* AiResearch Rep. AP-68-3249 (Data Item 55-10.02), Mar. 11, 1968. (Available as NASA CR-112279.)
93. *HREP—Phase IIA—Ground Support Equipment Development, First Interim Technical Data Report.* AiResearch Rep. AP-67-2830 (Data Item 55-10.01), Nov. 10, 1967. (Available as NASA CR-112280.)
94. *HREP—Phase IIA—Ground Support Equipment Development, Fourth Interim Technical Data Report.* AiResearch Rep. AP-68-4127 (Data Item 55-10.04), Aug. 6, 1968. (Available as NASA CR-112281.)
95. *HREP—Phase IIA—Ground Support Equipment Development, Third Interim Technical Data Report.* AiResearch Rep. AP-68-3731 (Data Item 55-10.03), May 3, 1968. (Available as NASA CR-112282.)
96. *HREP—Phase IIA—X15A-2 Integration Program, Fourth Interim Technical Data Report.* AiResearch Rep. AP-68-3794 (Data Item 55-9.04), May 31, 1968. (Available as NASA CR-112283.)
97. *HREP—Phase IIA—X15A-2 Integration Program, Final Technical Data Report.* AiResearch Rep. AP-68-4196 (Data Item 55-9.05), Aug. 28, 1968. (Available as NASA CR-112284.)

APPENDIX
(continued)

98. *HREP—Phase IIA—Structures Assembly Model Test Procedure.* AiResearch Rep. AP-70-6302 (Data Item 65.01), Jun. 23, 1970. (Available as NASA CR-112289.)
99. *HREP—Phase II—AiResearch Computer Program, H1760, Aerodynamic Heat Transfer Evaluation.* AiResearch Rep. AP-68-4530 (Data Item 54.09), Dec. 17, 1968. (Available as NASA CR-112290.)
100. *HREP—Phase IIA—SAM Temperature Control System Operation and Service Procedure.* AiResearch Rep. AP-70-6484 (Data Item 65.02), Aug. 31, 1970. (Available as NASA CR-112291.)
101. *HREP—Phase IIA—Aerodynamic and Engine Performance Analysis, First Interim Technical Data Report.* AiResearch Rep. AP-67-2831 (Data Item 55-11.01), Nov. 20, 1967. (Available as NASA CR-132326.)
102. *HREP—Phase IIA—Aerodynamic and Engine Performance Analysis, Second Interim Technical Data Report.* AiResearch Rep. AP-67-3133 (Data Item 55-11.02), Feb. 13, 1968. (Available as NASA CR-132327.)
103. *HREP—Phase IIA—Aerodynamic and Engine Performance Analysis, Third Interim Technical Data Report.* AiResearch Rep. AP-68-3752 (Data Item 55-11.03), May 13, 1968. (Available as NASA CR-132328.)
104. *HREP—Phase IIA—Aerodynamic and Engine Performance Analysis, Terminal Summary Report.* AiResearch Rep. AP-68-4490 (Data Item 55-11.05), Dec. 5, 1968. (Available as NASA CR-132329.)
105. *HREP—Phase IIA—Aerodynamic and Engine Performance Analysis, Fourth Interim Technical Data Report.* AiResearch Rep. AP-68-4017 (Data Item 55-11.04), Jul 31, 1968. (Available as NASA CR-132330.)
106. *HREP—Phase II—Aerothermodynamic Integration Model Test Plan.* AiResearch Rep. AP-71-7877 (Data Item 2-2.01), May 26, 1972. (Available as NASA CR-132497.)
107. *HREP—Phase II—Aerothermodynamic Integration Model Measurement Plan.* AiResearch Rep. AP-70-6216 (Data Item 2-1.01), Jun. 9, 1970. (Available as NASA CR-132498.)
108. *HREP—Phase II—Some Combustor Test Results of NASA Aerothermodynamic Integration Model.* AiResearch Rep. AP-74-10818 (Data Item 54.14), Sept. 26, 1974. (Available as NASA CR-132525.)
109. *HREP—Phase IIA—Nozzle Program, Fourth Interim Technical Data Report.* AiResearch Rep. AP-68-3960 (Data Item 55-3.04), Jul. 10, 1968. (Available as NASA CR-132534.)
110. *HREP—Phase II—Preliminary Report on the Performance of the HRE/AIM at Mach 6.* AiResearch Rep. AP-74-10951 (Data Item 54.15), Nov. 6, 1974. (Available as NASA CR-132538.)
111. *HREP—Phase IIA—Overall Summary Test Plan.* AiResearch Rep. AP-67-1869 (Data Item 1.04), Oct. 27, 1967. (Available as NASA CR-132539.)
112. *HREP—Phase II—Aerothermodynamic Integration Model Development, Twentieth Interim Technical Data Report.* AiResearch Rep. AP-73-9154 (Data Item 55-4.20), Mar. 9, 1973. (Available as NASA CR-132540.)
113. *HREP—Phase II—Aerothermodynamic Integration Model Development, Nineteenth Interim Technical Data Report.* AiResearch Rep. AP-72-8916 (Data Item 55-4.19), Dec. 9, 1972. (Available as NASA CR-132541.)
114. *HREP—Phase I—Computer Program Description Ramjet and Scramjet Cycle Performance.* AiResearch Rep. AP-1001-1, Dec., 1965. (Available as NASA CR-132454.)
115. *HREP—Phase I—Engine Development Plan, Technical Proposal for Phase II.* AiResearch Rep. AP-66-0169, Feb. 28, 1965. (Available as NASA CR-132542.)
116. *HREP—Phase IIA—Instrumentation Program, First Interim Technical Data Report.* AiResearch Rep. AP-67-2203 (Data Item 55-8.01), Jun. 7, 1967. (Available as NASA CR-132591.)
117. *HREP—Phase IIA—Instrumentation Program, Second Interim Technical Data Report.* AiResearch Rep. AP-67-2579 (Data Item 55-8.02), Sept. 25, 1967. (Available as NASA CR-132592.)

APPENDIX
(continued)

118. *HREP—Phase IIA—Instrumentation Program, Third Interim Technical Data Report.* AiResearch Rep. AP-67-3020 (Data Item 55-8.03), Dec. 21, 1967. (Available as NASA CR-132593.)
119. *HREP—Phase IIA—Instrumentation Program, Fourth Interim Technical Data Report.* AiResearch Rep. AP-68-3429 (Data Item 55-8.04), Apr. 10, 1968. (Available as NASA CR-132594.)
120. *HREP—Phase IIA—Instrumentation Program, Fifth Interim Technical Data Report.* AiResearch Rep. AP-68-3847 (Data Item 55-8.05), Jun. 12, 1968. (Available as NASA CR-132595.)
121. *HREP—Phase IIA—Instrumentation Program, Sixth Interim Technical Data Report.* AiResearch Rep. AP-68-4273 (Data Item 55-8.06), Sept. 27, 1968. (Available as NASA CR-132596.)
122. *HREP—Phase IIA—Instrumentation Program, Terminal Summary Report.* AiResearch Rep. AP-68-3953 (Data Item 55-8.07), Oct. 22, 1968. (Available as NASA CR-132597.)
123. *HREP—Phase IIA—Nozzle Program, First Interim Technical Data Report.* AiResearch Rep. AP-67-2583 (Data Item 55-3.01), Sept. 27, 1967. (Available as NASA CR-132590.)
124. *HREP—Phase IIA—Nozzle Program, Second Interim Technical Data Report.* AiResearch Rep. AP-67-3129 (Data Item 55-3.02), Jan. 11, 1968. (Available as NASA CR-132589.)
125. *HREP—Phase IIA—Nozzle Program, Third Interim Technical Data Report.* AiResearch Rep. AP-68-3587 (Data Item 55-3.03), Apr. 8, 1968. (Available as NASA CR-132588.)
126. *HREP—Phase IIA—Environmental Specification.* AiResearch Rep. AP-68-4130 (Data Item 4.02), Aug. 14, 1968. (Available as NASA CR-132599.)
127. *HREP—Phase IIA—Instrumentation Development Plan.* AiResearch Rep. AP-67-2545 (Data Item 14.01), Dec. 13, 1967. (Available as NASA CR-132598.)
128. *HREP—Phase II—Aerothermodynamic Integration Model Development—Seventeenth Interim Technical Data Report.* AiResearch Rep. AP-72-8542 (Data Item 55-4.17), Jun. 27, 1972. (Available as NASA CR-132585.)
129. *HREP—Phase II—Structures Assembly Model Test Plan.* AiResearch Rep. AP-70-6120 (Data Item 64.01), Mar. 11, 1970. (Available as NASA CR-132600.)
130. *HREP—Phase II—Aerothermodynamics Integration Model Development. Final Technical Data Report.* AiResearch Rep. AP-75-11133 (Data Item 55-4.21), May 19, 1975. (Available as NASA CR-132654.)
131. *HREP—Phase II—Aerothermodynamics Integration Model AIM Test Report.* AiResearch Rep. AP-74-10784 (Data Item 63.06), May 19, 1975. (Available as NASA CR-132655.)
132. *HREP—Phase II—Aerothermodynamics Integration Model Data Reduction Computer Program.* AiResearch Rep. AP-75-11502 (Data Item 54.16), May 16, 1975. (Available as NASA CR-132656.)

Miscellaneous Published Reports

133. Andrews, Earl H. Jr., and Rogers, R. Clayton: *Study of Underexpanded Exhaust Jets of an X-15 Airplane Model and Attached Ramjet Engine Simulator at Mach 6.86.* NASA TM X-1571, May 1968.
134. Andrews, Earl H.; and Mackley, Ernest A.: *Analysis of Experimental Results of the Inlet for the NASA Hypersonic Research Engine Aerothermodynamic Integration Model.* NASA TM X-3365, 1976.
135. Andrews, Earl H., Jr.; Mackley, Ernest A.; and Engineering Staff of AiResearch Manufacturing Co.: *Hypersonic Research Engine/Aerothermodynamic Integration Model Experimental Results. Vol. I—Mach 6 Component Integration.* NASA TM X-72821, 1976.
136. Andrews, Earl H., Jr.; Mackley, Ernest A.; and Engineering Staff of AiResearch Manufacturing Co.: *Hypersonic Research Engine/Aerothermodynamic Integration Model Experimental Results. Vol. II—Mach 6 Performance.* NASA TM X-72822, 1976.

APPENDIX
(continued)

137. Andrews, Earl H., Jr.; Mackley, Ernest A.; and Engineering Staff of AiResearch Manufacturing Co.: *Hypersonic Research Engine/Aerothermodynamic Integration Model Experimental Results. Vol. III—Mach 7 Component Integration and Performance.* NASA TM X-72823, 1976.
138. Andrews, Earl H., Jr.; Mackley, Ernest A.; and Engineering Staff of AiResearch Manufacturing Co.: *Hypersonic Research Engine/Aerothermodynamic Integration Model Experimental Results. Vol. IV—Mach 5 Component Integration and Performance.* NASA TM X-72824, 1976.
139. Andrews, Earl H., Jr.; Russell, James W.; Mackley, Ernest A.; and Simmonds, Ann L.: *An Inlet Analysis for the NASA Hypersonic Research Engine Aerothermodynamic Integration Model.* NASA TM X-3038, 1974.
140. Andrews, Earl H., Jr.; McClinton, Charles R.; and Pinckney, S. Z.: *Flow Field and Starting Characteristics of an Axisymmetric Mixed Compression Inlet.* NASA TM X-2072, 1971.
141. Bahn, Gilbert S.: *Calculations of the Autoignition of Mixtures of Hydrogen and Air.* LVT Contract NAS1-10900. NASA CR-112067, 1972.
142. Bahn, Gilbert S.: *Approximate Thermochemical Tables for Some C-H and C-H-O Species.* LTV Aerospace Corp. NAS1-10900. NASA CR-2178, 1973.
143. Bahn, Gilbert S.: *Theoretical Nitric Oxide Production Incidental to Autoignition and Combustion of Several Fuels Homogeneously Dispersed in Air Under Some Typical Hypersonic Flight Conditions.* LTV Aerospace Corp. NAS1-10900. NASA CR-2455, 1974.
144. Carson, G. T., Jr.: *Analytical Chemical Kinetic Investigation of the Effects of Oxygen, Hydrogen, and Hydroxyl Radicals on Hydrogen-Air Combustion.* NASA TN D-7769, 1974.
145. Lezberg, Erwin A.; Pack, William D.; and Metzler, Allen J.: *In-Stream Measurements of Combustion During Mach 5-7 Tests of the Hypersonic Research Engine (HRE).* AIAA 93-2324, 1993.
146. Molloy, John K.; Mackley, Ernest A.; and Keyes, J. Wayne: *Effect of Diffusers, Shrouds, and Mass Injection on the Starting and Operating Characteristics of a Mach 5 Free Jet Tunnel.* NASA TN D-6377.
147. Research Staffs of NASA Langley Research Center and AiResearch Manufacturing Division: *HREP Technological Status 1971 (NAS1-6666.)* NASA TM X-2572, 1972.
148. Wieting, Alan R.: *Aerodynamic and Thermal Analysis of Results of Tests of a Hydrogen-Cooled Scramjet Engine at Mach 6.3.* NASA TM X-2767, 1973.
149. Weiting, A. R.: *Experimental Blockage Study of a Ramjet Engine (HRE-AIM) Using the Langley 7-Inch Mach 7 Pilot Tunnel.* NASA/Langley Research Center, Hampton, VA. Report No. LWP-888, Aug. 1970. (Available from author only.)
150. Gaede, A. E.; and Lopez, H. J.: *Selection of Nozzle Contours For a Research Scramjet Engine.* AIAA 67-453, 1967.
151. Kuo, K. K.; and Sun, Y. H. Pan: *A Simplified Flow-Field Analysis of a Two-Dimensional or Axisymmetric Supersonic Combustor.* AIAA 67-494, 1967.
152. Mackley, Ernest A.: *NASA's Hypersonic Research Engine Project.* AIAA 3rd Propulsion Joint Specialists Conference, July 17-21, 1967.
153. Benson, John L.: *Scramjet Induction System Development.* AIAA 3rd Propulsion Joint Specialists Conference, July 17-21, 1967.
154. Andersen, Lee; and Sun, Y. H.: *Experimental Investigation of Hydrogen Autoignition Qualities in Supersonic Combustion Chambers.* AIAA 3rd Propulsion Joint Specialists Conference, July 17-21, 1967.
155. Buchmann, O. A.; Fliedler, W. G.; and Walters, F.: *Application of Regeneratively Cooled Flat Panels Study to the X-15 Hypersonic Research Engine.* AIAA 3rd Propulsion Joint Specialists Conference, July 17-21, 1967.

APPENDIX
(concluded)

156. Lopez, Henry J.: *Hypersonic Research Engine Aerodynamic Design*. AIAA 5th Propulsion Joint Specialists Conference, June 9-13, 1969.
157. Flieder, W. G.; Richard, C. E.; Young, C. F.; and Walters, F. M.: *Hypersonic Research Engine Structures and Cooling*. AIAA 5th Propulsion Joint Specialists Conference, June 9-13, 1969.
158. Benson, J. L.; Miller, L. D.; Santman, D. M.; Mackley, E. A.; and Pearson, L. W.: *Hypersonic Research Engine Inlet Development Program*. AIAA 5th Propulsion Joint Specialists Conference, June 9-13, 1969.
159. Short, Gordon R.; Sotter, J. G.; and Sun, Y. H.: *Hypersonic Research Engine Combustor Development Program*. AIAA 5th Propulsion Joint Specialists Conference, June 9-13, 1969.
160. Pearson, Lowell W.; and Gaede, A. E.: *Hypersonic Research Engine Project: Exhaust Nozzle Development Program*. AIAA 5th Propulsion Joint Specialists Conference, June 9-13, 1969.
161. Lopez, Henry J.; and Rubert, Kennedy F.: *Progress and Status of NASA Hypersonic Engine Project*. AIAA/SAE 7th Propulsion Joint Specialists Conference, June 14-18, 1971. (Also available as NASA HRE Project: A Review of Progress. Henry J. Lopez and Kennedy F. Rubert; NASA CR-104173, 1967.)
162. Kelly, H. N.; and Vuigner, Anthony A.: *High Temperature Tests of a Hypersonic Regeneratively Cooled Engine Structure*. AIAA/SAE 7th Propulsion Joint Specialists Conference, June 14-18, 1971.
163. Sun, Yung H.; and Sainio, Walter C.: *Experimental Results of Supersonic Combustion and its Application to Combustor Design*. AIAA/SAE 7th Propulsion Joint Specialists Conference, June 14-18, 1971.
164. Buchmann, O. A.: *Design of Actively Cooled Hypersonic Engine Structures*. AIAA/SAE 7th Propulsion Joint Specialists Conference, June 14-18, 1971.

REFERENCES

1. Mackley, Ernest A.: NASA Hypersonic Research Engine Project. AIAA Third Propulsion Joint Specialist Conference, Washington, DC, July 17-21, 1967.
2. Henry, John R.; Mackley, Ernest A.; and Torrence, Marvin G.: Investigation of the Compression Field and the Flow Distribution in the Throat of a Two-Dimensional, Internal-Compression, Mach 6.9 Inlet. NASA TM X-605, November 1961.
3. Anderson, Griffin Y.: Supersonic Combustion Ramjet performance. NASA TM X-968, May 1964.
4. Henry, John R.: Fuel Injection and Mixing in Scramjet Combustors. NASA TM X-1437, Oct. 1967.
5. Sanlorenzo, E., et al.: Scramjet Experimental Flight Test Program. AF APL TR-67-112.
6. Kenworthy, M. J.: Analytical and Experimental Evaluation of the Supersonic Combustion Ramjet Engine. AF APL-TR-65-103, General Electric Co., Evendale, Ohio.
7. McFarlin, David J.; and Kepler, C. Edward: Mach 5 Test Results of Hydrogen-Fueled Variable-Geometry Scramjet. United Aircraft Research Laboratories Technical Report AF APL-TR-68-116.
8. HREP - Phase IIA - Fuel System Development. Terminal Summary Report, AiResearch Report No. APP-68-4611, December 17, 1968, Data Item 55-5.08, NASA CR -111902.
9. HREP - Phase IIA - Control System Development. Terminal Summary Report, AiResearch Report No. AP-68-4540, April 16, 1969, Data Item 55-6.06, NASA CR-111900.
10. HREP - Phase IIA - Fuel System Turbopump Development. Terminal Summary Report, AiResearch Report No. AP-68-4472, November 4, 1968, Data Item 55-5.07, NASA CR-111900.
11. HREP - Phase IIA - X-15A-2 Integration Program. Final Technical Data Report, AiResearch Report No. AP-68-4196, August 28, 1968, Data Item 55-9.05, NASA CR-112284.
12. HREP - Phase IIA - Instrumentation Program. Terminal Summary Report, AiResearch Report No. AP-68-3953, October 22, 1968, Data Item 55-8.07, NASA CR -132597.
13. HREP - Phase IIA - Ground Support Equipment Development. Terminal Summary Report, AiResearch Report No. AP-68-4301, September 26, 1968, Data Item 55-10.05, NASA CR-112276.
14. Hube, Frederick K.: Tests of a One-Third Scale NASA Hypersonic Research Engine Inlet at Mach Numbers 6 and 8. AEDC-TR-68-28, March 1968.
15. Hube, Frederick K.; and Bontrager, Paul J.: Wind Tunnel Tests of a Two-Thirds Scale NASA HRE Inlet at Mach Numbers 4, 5, 6, and 8. AEDC-TR-69-9, February 1969.
16. HREP - Phase IIA - Inlet Program. Terminal Summary Report, AiResearch Report No. AP-69-4883, March 27, 1969, Data Item 55-1.08, NASA CR-66797.

17. Andrews, Earl H., Jr.; McClinton, Charles R.; and Pinckney, S. Z.: Flow Field and Starting Characteristics of an Axisymmetric Mixed Compression Inlet. NASA Langley Research Center, January 1971, NASA TM X-2072.
18. HREP - Phase II - Combustor Program. Final Technical Data Report, AiResearch Report No. AP-70-6054, March 23, 1970, Data Item 55-2.11, NASA CR-66932.
19. Kay, I. W.; and McVey, J. R.: Hydrocarbon Fueled Scramjet-Wall Divergence Investigation. AF APL-TR-68-146, vol. X, USAF, Dec. 1971.
20. HREP - Phase IIA - Nozzle. Terminal Summary Report, AiResearch Report No. AP-68-4451, December 17, 1968, Data Item 55-3.05, NASA CR-101532.
21. HREP - Phase II - Structures and Cooling Development. Final Technical Data Report. AiResearch Report No. AP-72-8237, May 18, 1972, Data Item 55-7.18, NASA CR-112087.
22. HREP - Phase II - Structures Assembly Model Test Report Data. AiResearch Report No. AP-71-7702, September 22, 1971, Data Item 63.05, NASA CR-111993.
23. Wieting, Alan R.: Aerodynamic and Thermal Analysis of Results of Tests of a Hydrogen Cooled Scramjet Engine at Mach 6.3. NASA TM X-2767, May 1973.
24. Deveikis, William D., and Hunt, L. Roane: Loading and Heating of a Large Flat Plate at Mach 7 in the Langley 8-Foot High-Temperature Structures Tunnel. NASA TN D-7275, Sept. 1973.
25. Cullom, Richard R.; and Lezberg, Erwin A.: Calibration of Lewis Hypersonic Tunnel Facility at Mach 5.6 and 7. NASA TN D-7100, 1972.
26. Andersen, W. L.; and Kado, K.: HREP - Phase II - Aerothermodynamics Integration Model Test Report. AiResearch Report No. AP-74-10784, May 19, 1975, Data Item 63.06, NASA CR-132655.
27. HREP - Phase II - Aerothermodynamics Integration Model Development. Final Technical Data Report. AiResearch Report No. AP-75-11133, May 19, 1975, Data Item 55-4.21, NASA CR-132654.
28. Andrews, Earl H., Jr.; Mackley, Ernest A.; and Engineering Staff, AiResearch Manufacturing Co.: Hypersonic Research Engine/Aerothermodynamic Integration Model Experimental Results. April 1976.
 Vol. I - Mach 6 Component Integration. NASA TM X-728821.
 Vol. II - Mach 6 Performance. NASA TM X-72822.
 Vol. III - Mach 7 Component Integration and Performance. NASA TM X-72823.
 Vol. IV - Mach 5 Component Integration and Performance. NASA TM X-72824.
29. Lezberg, Erwin A.; Pack, William D., and Metzler, Allen J.: In-Stream Measurements of Combustion During Mach 5-7 Tests of the Hypersonic Research Engine (HRE). AIAA Paper 93-2324, June 1993.
30. Andrews, Earl H., Jr.; Russell, James W.; Mackley, Ernest A.; and Simmonds, Ann L.: An Inlet Analysis for the NASA Hypersonic Research Engine Aerothermodynamic Integration Model. NASA TM X-3038, November 1974.
31. Andrews, Earl H.; and Mackley, Ernest A.: Analysis of Experimental Results of the Inlet for the NASA Hypersonic Research Engine Aerothermodynamic Integration Model. NASA TM X-3365, June 1976.

32. Becker, John V.: **Confronting Scramjet: The NASA Hypersonic Ramjet Experiment. Case VI in the Hypersonic Revolution: Eight Case Studies in the History of Hypersonic Technology; Vol. II - From Scramjet to the National Aero-Space Plane (1964-1986)**, edited by Richard P. Hallion with contributions by John V. Becker, Richard Hallion, John Vitelli, and James Young. A special Staff Office Study, Aeronautical Systems Division, Wright-Patterson Air Force Base, Ohio, 1987.

Table I. SAM Tunnel Tests.
Thermal fatigue summary

Tunnel total conditions		Number of cycles	Time in stream, (sec)	Avg cycle temperatures		Calculated damage fraction, %
P _{t,0} , psia	T _{t,0} , °R			T _{max} , °R	Δ T, °F	
950	2600	5	172	1360	733	1.30
1300	2700	3	135	1445	950	2.12
1380	2700	33	851	1446	906	20.50
1500	2700	3	138	1571	1152	3.77
2200	3000	5	266	1591	1287	8.36
2800	3300	1	58	1435	1224	1.19
3300	3400	5	163	1522	1350	8.46
Totals		55	1783	—		45.70

● Test period 29.7 min

EAMN198714AAA

- Test period
- 1971-1972

Table II. AIM Test Summary.

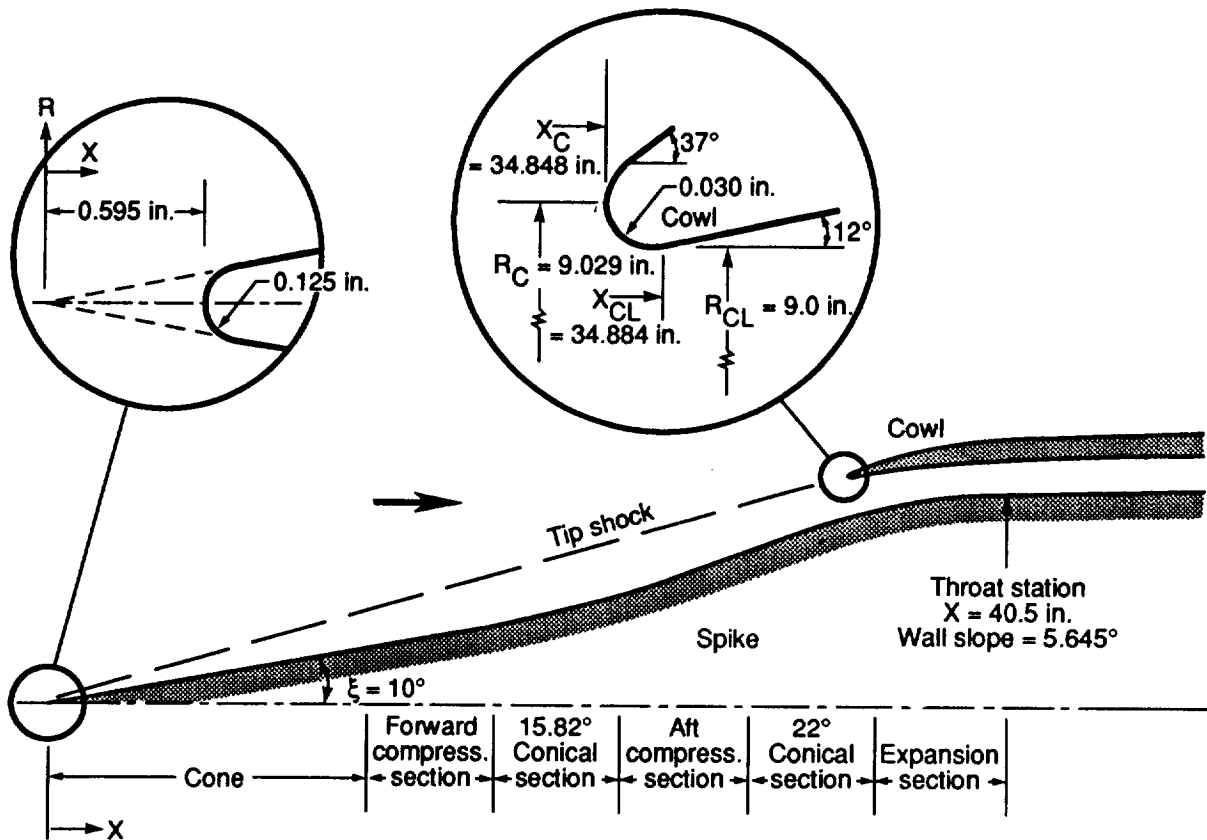
Mach No.	No. of Tests	Time at test cond (min/sec)	P _{t,0} (psia)	T _{t,0} (°R)
5	5	19' 30"	210/415	2210/3000
6	36	63' 17"	466/750/930	1500/3000
7	11	28' 57"	1000	3000/3500
52		111' 44"		

EAMN198714AAA

- Test period
 - Mach 6 from Oct 5, 1973 to Dec 19, 1973
 - Mach 7 from Jan 22, 1974 to Mar 18, 1974
 - Mach 5 from Mar 20, 1974 to Apr 22, 1974

Table III. HRE-AIM Configuration.
(Mach 6 design cowl position, $X_C = 34.848$ in.)

a) Schematic



b) Coordinates

Spike			
X/R _{CL}	R/R _{CL}	X/R _{CL}	R/R _{CL}
0.066	0.0	3.787	0.793
0.077	0.014	4.190	0.956
2.040	0.360	4.230	0.971
2.145	0.379	4.274	0.984
2.271	0.404	4.308	0.991
2.410	0.432	4.341	0.997
2.537	0.458	4.374	1.003
2.650	0.482	4.408	1.087
2.875	0.531	4.411	1.013
2.974	0.554	4.500	1.020
3.100	0.584	4.602	1.030
3.212	0.613	4.659	1.035
3.295	0.636	4.714	1.040
3.373	0.658	5.378	1.074
3.640	0.740	6.196	1.074

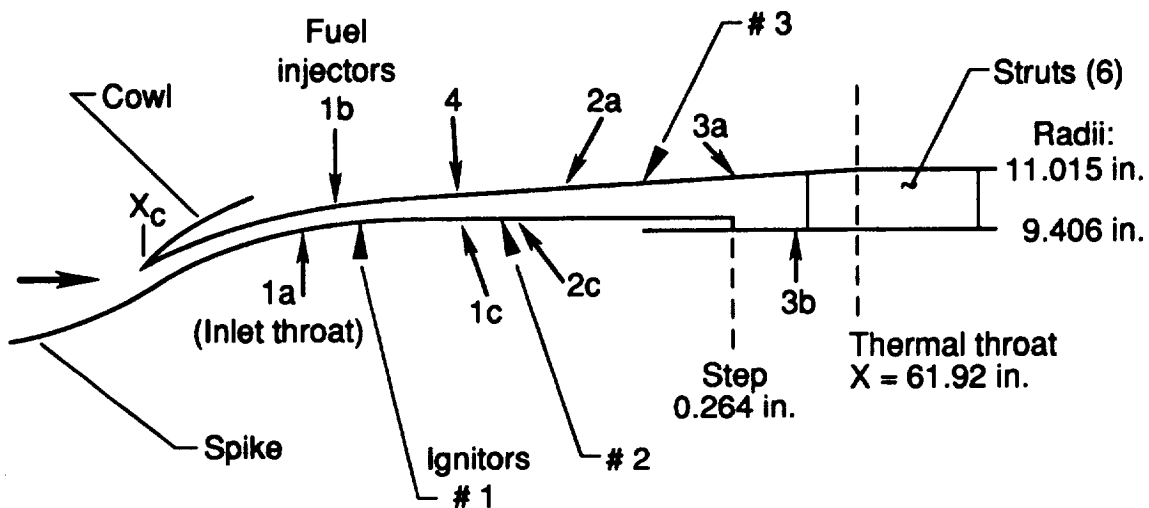
Notes for Spike table:
 - X/R_{CL} 0.066 to 2.974: Straight line, $\xi = 10.0^\circ$
 - X/R_{CL} 2.974 to 4.411: Straight line, $\xi = 15.819^\circ$
 - X/R_{CL} 4.411 to 4.500: Throat
 - X/R_{CL} 4.500 to 4.714: Straight line, $\xi = 0^\circ$
 - X/R_{CL} 4.714 to 6.196: Straight line, $\xi = 22.0^\circ$

Cowl		
X/R _{CL}	R/R _{CL}	
3.872	1.003	$\xi = 90^\circ$
3.876	1.0	$\xi = 12^\circ$
3.933	1.012	
3.986	1.021	$\xi = 10^\circ$
4.019	1.027	
4.046	1.031	$\xi = 8^\circ$
4.085	1.036	
4.166	1.044	Straight line
5.326	1.159	$\xi = 5.645^\circ$
6.196	1.203	

Table IV. HRE-AIM Combustor Configuration.

[Mach 6 design cowl position, $X_C = 34.848$ in.]

a) Schematic



b) Fuel Injector Parameters

Designation (a)	Number of injectors	Orifice diameter, d, in.	Injection angle, deg. (b)	Peripheral spacing, s/d	M = 6 designed X-location in.
Fuel injectors					
1a	37 } ^e	0.119	90	13.1	40.50
1b			90	13.9	41.25
1c			106	13.5	44.50
4	37 } ^f	0.119	90	14.2	44.50
2a			67	11.4	48.50
2c	60 } ^f	0.095	119	10.6	46.50
3a	105 } ^f	0.090	120	7.0	53.75
3b			90	6.3	44.90
Ignitors					
Ignitor 1 ^c	6		94.5	} Equally spaced	42.00
Ignitor 2 ^c	6		120.0 ^d		45.50
Ignitor 3 ^c	6		60.0		51.00

^a Designations used in all HRE documentation

^b With respect to AIM center line in the view shown in the sketch

^c Gaseous hydrogen and oxygen torches

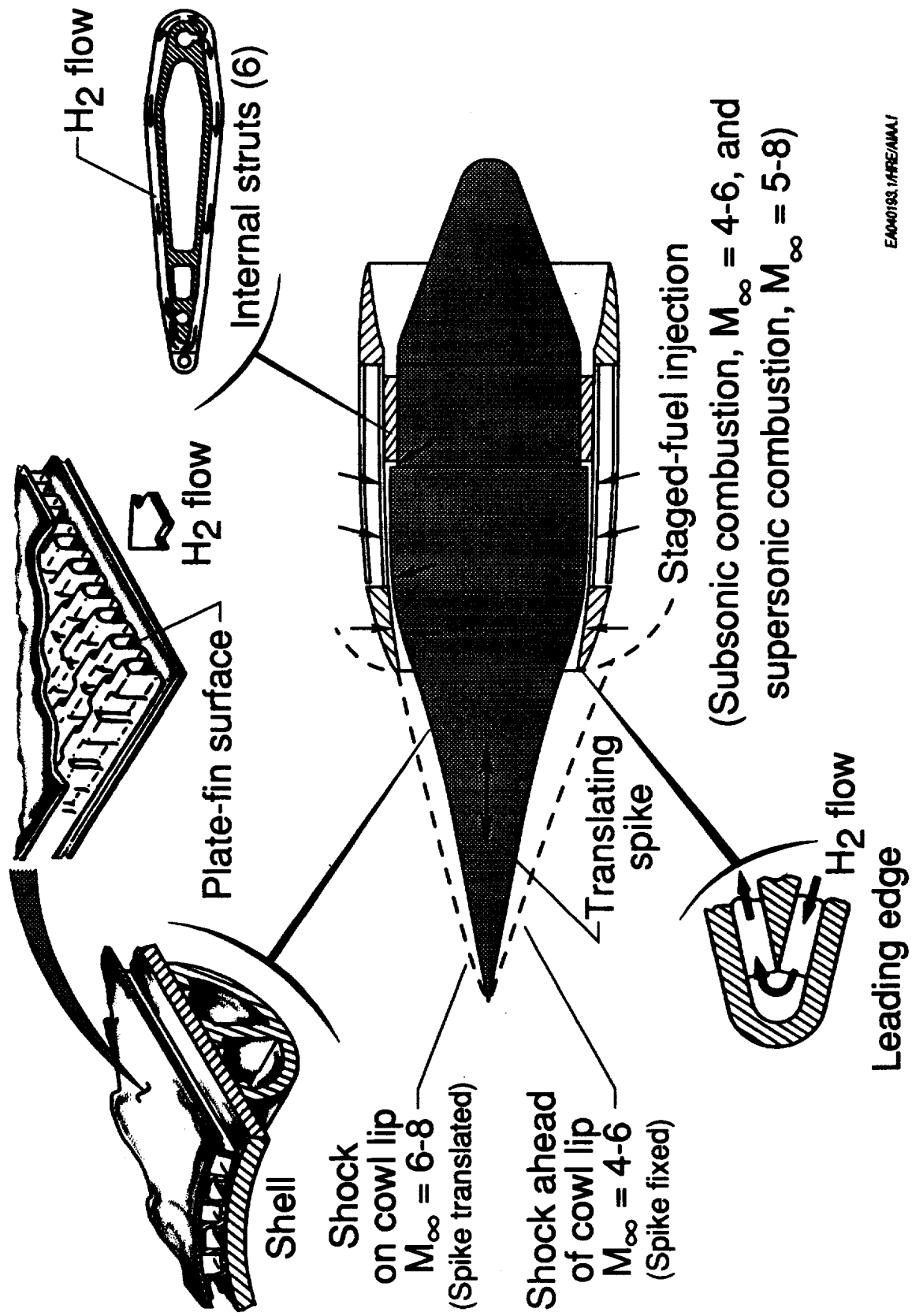
^d Also inclined at a 30° circumferential angle

^e Orifices inline

^f Orifices interdigitated

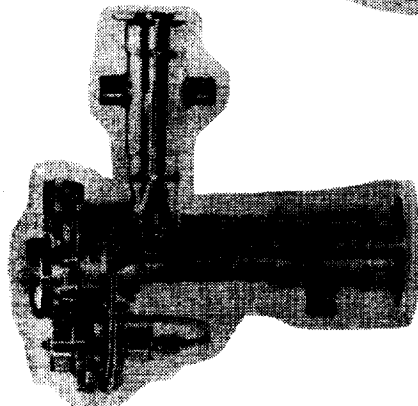


Figure 1.- Artist's concept of the HRE on the X-15A-2 aircraft just after launch from a B-52.

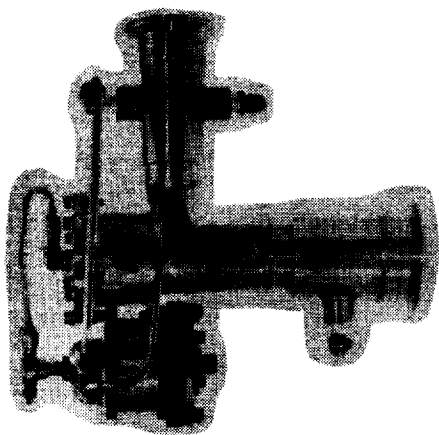


EA00193.1/ARE/AAJ

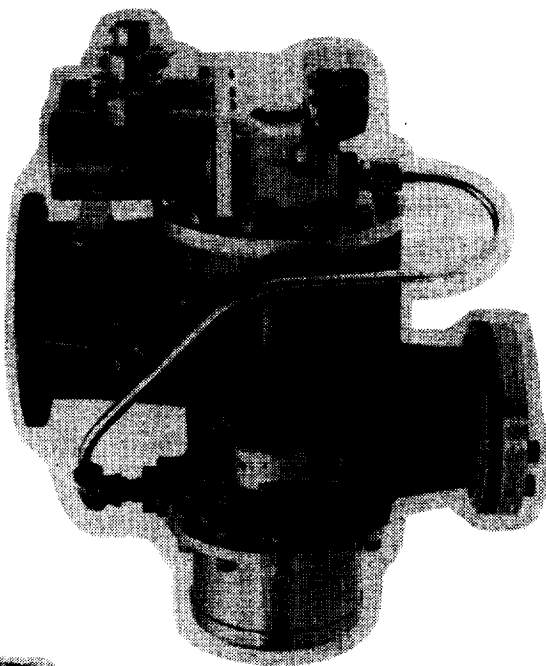
Figure 2.- Hypersonic Research Engine concept and flight engine design features.



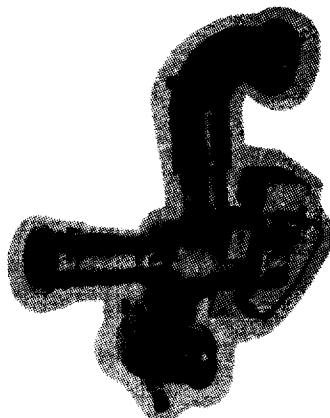
Turbine control



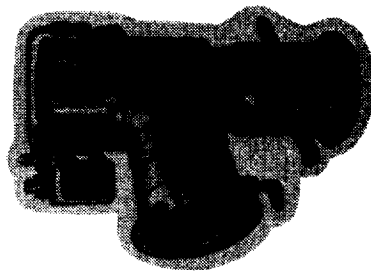
Coolant regulating



Purge and shutoff



Fuel control



Fuel dump

a) Regulating and control valves.

Figure 3.- Hydrogen system hardware.



Turbopump main housing



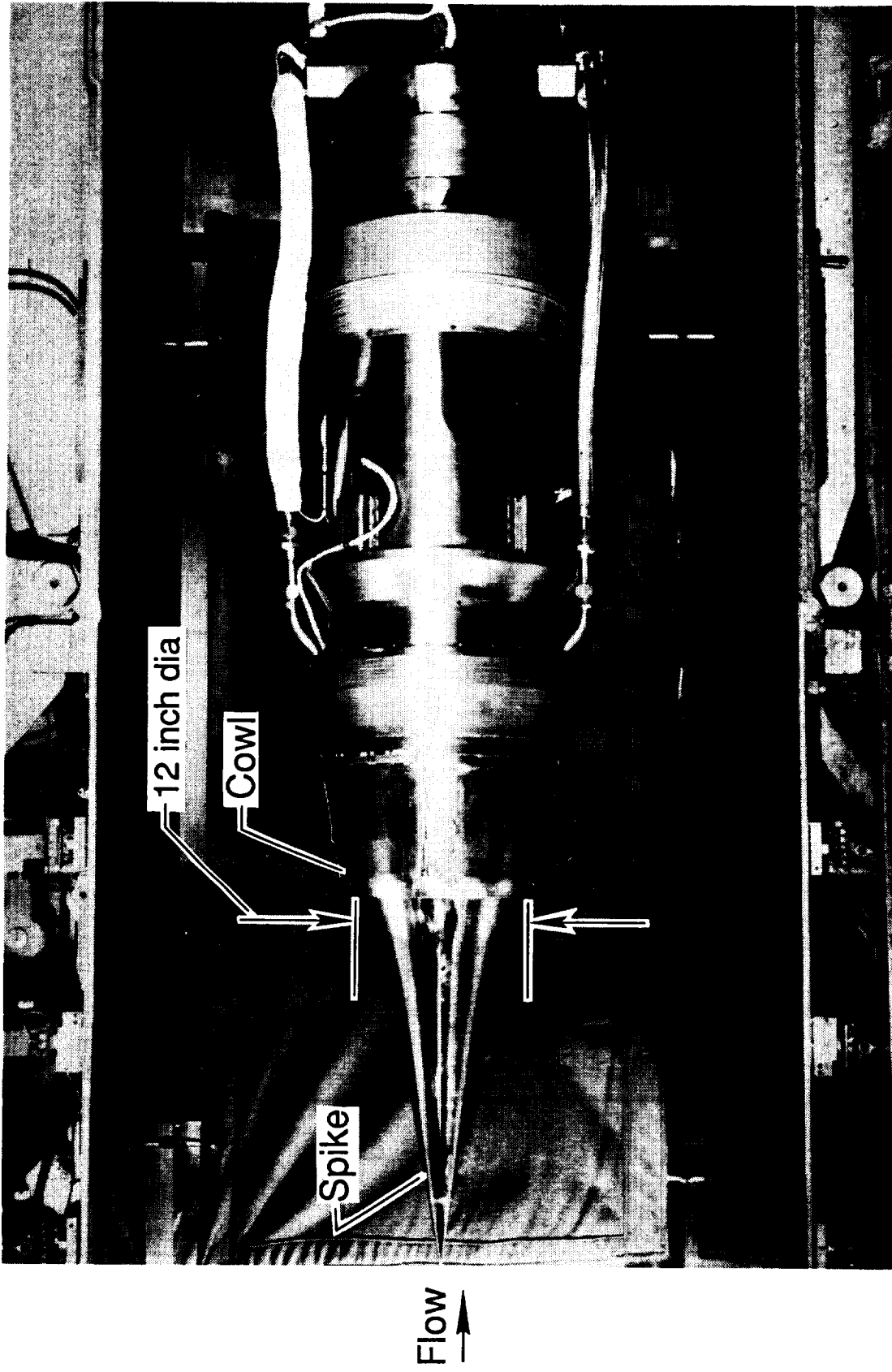
Turbopump impeller (open)



Turbopump impeller (shrouded)

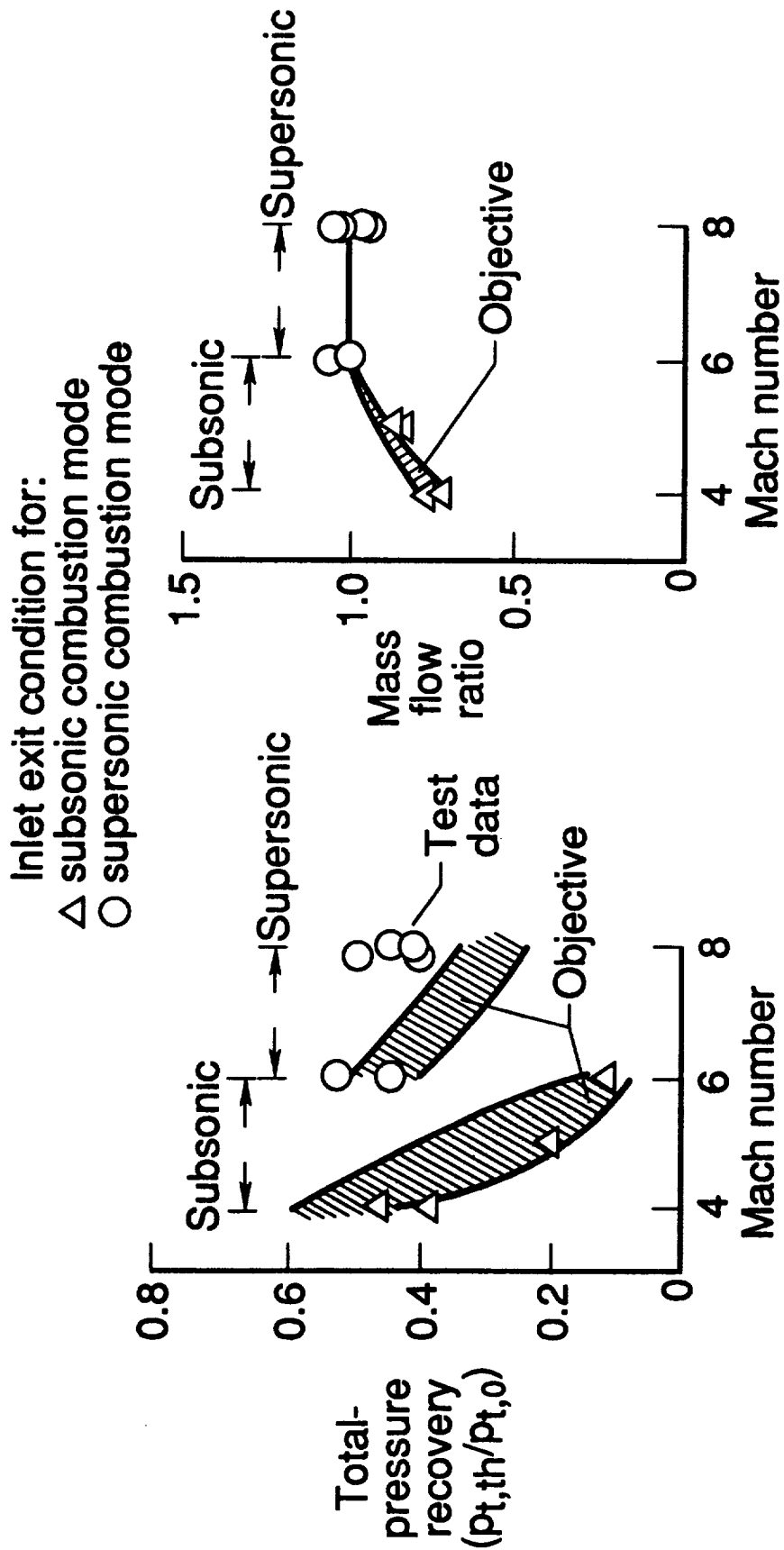
b) Hydrogen system turbopump.

Figure 3.- Concluded.



a) Model installed in Tunnel A, von Karman Facility of the Arnold Engineering Development Center.

Figure 4.- Inlet model and experimental performance; two-thirds scale model.

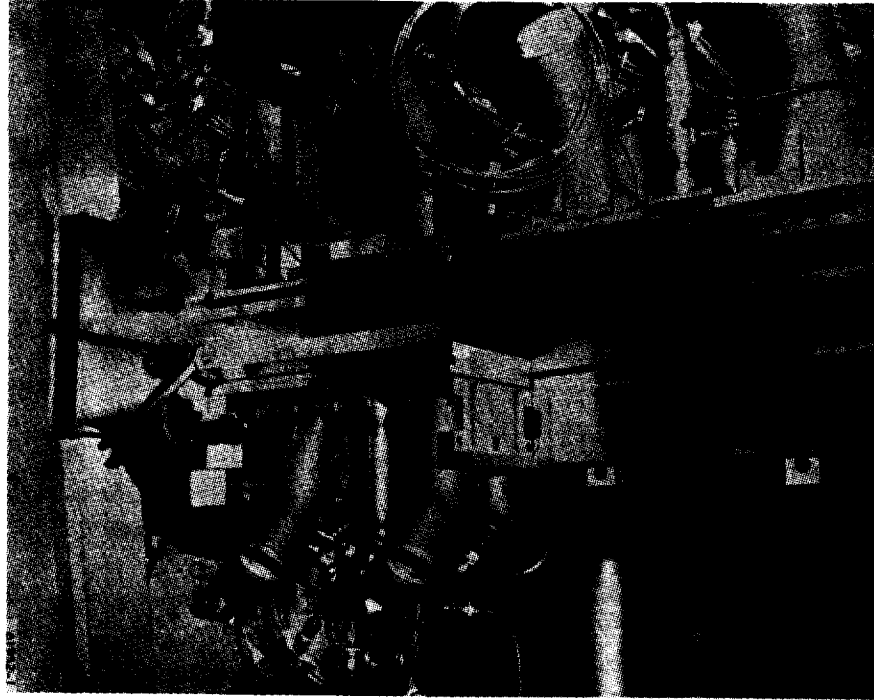


EA051000.1

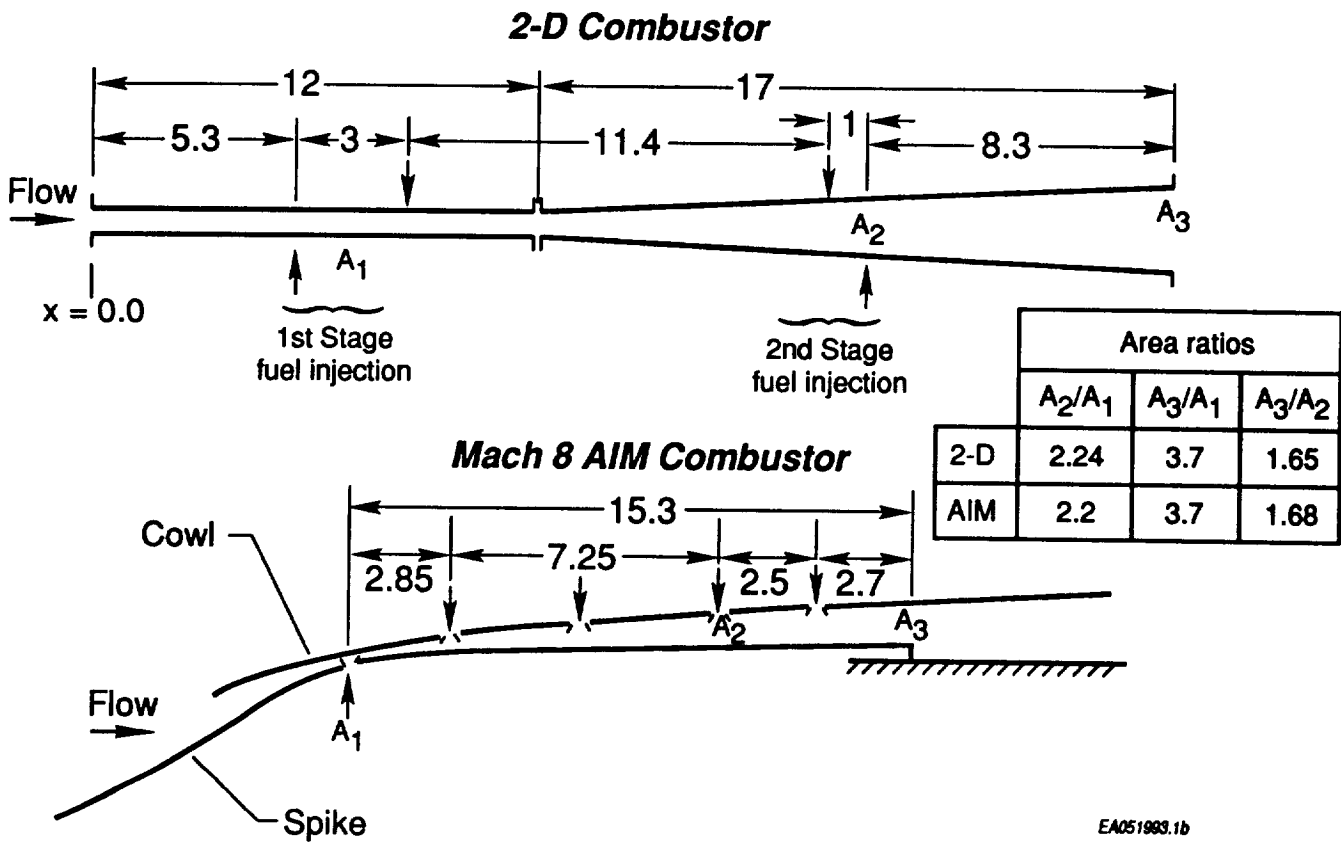
b) Inlet total-pressure recovery.

c) Inlet mass flow ratio schedule.

Figure 4. - Concluded.

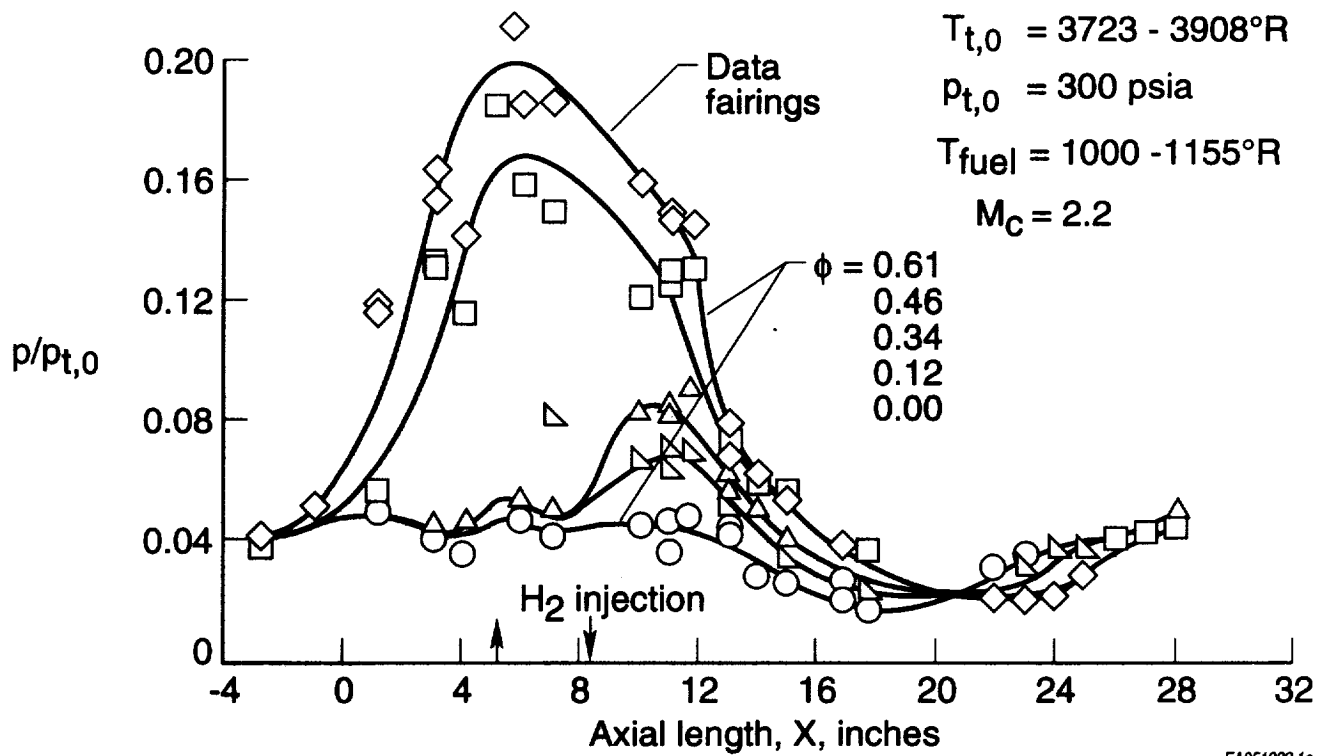


a) Partially assembled model.



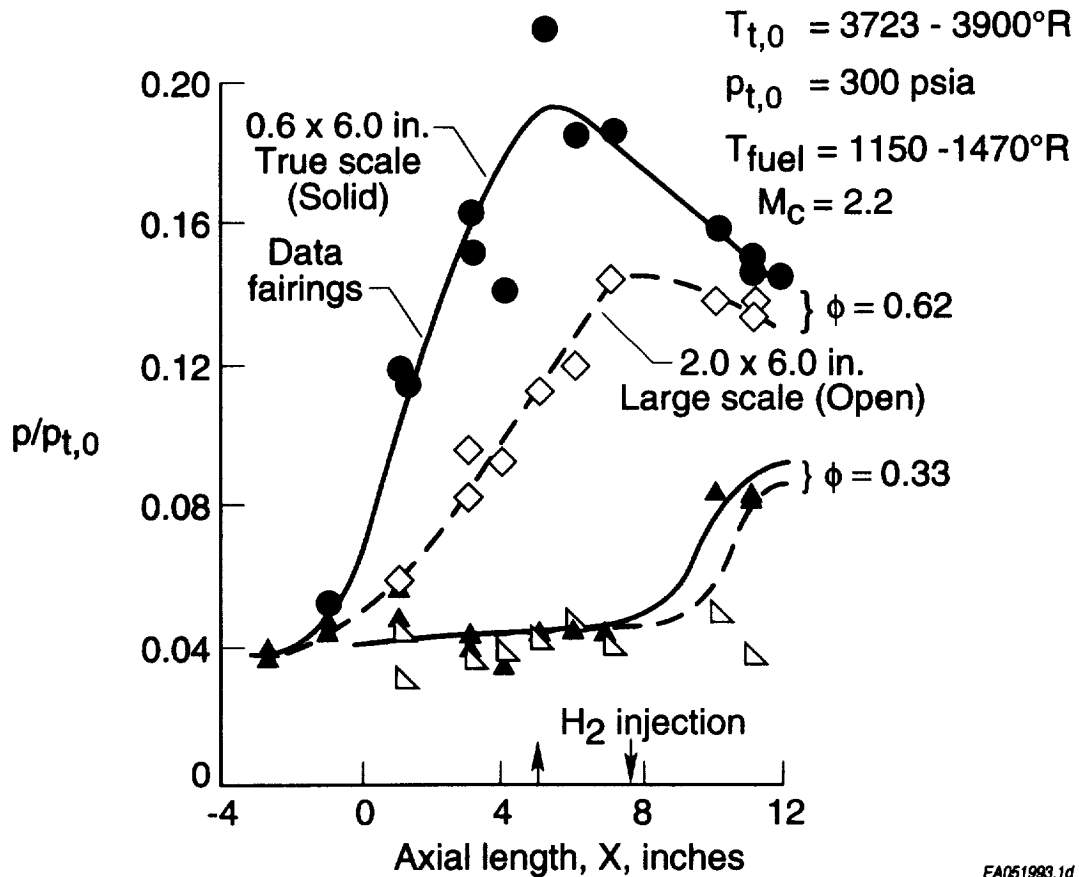
b) 2-D simulation of axisymmetric engine combustor; all dimensions in inches.

Figure 5.- Two-dimensional combustor model test program.



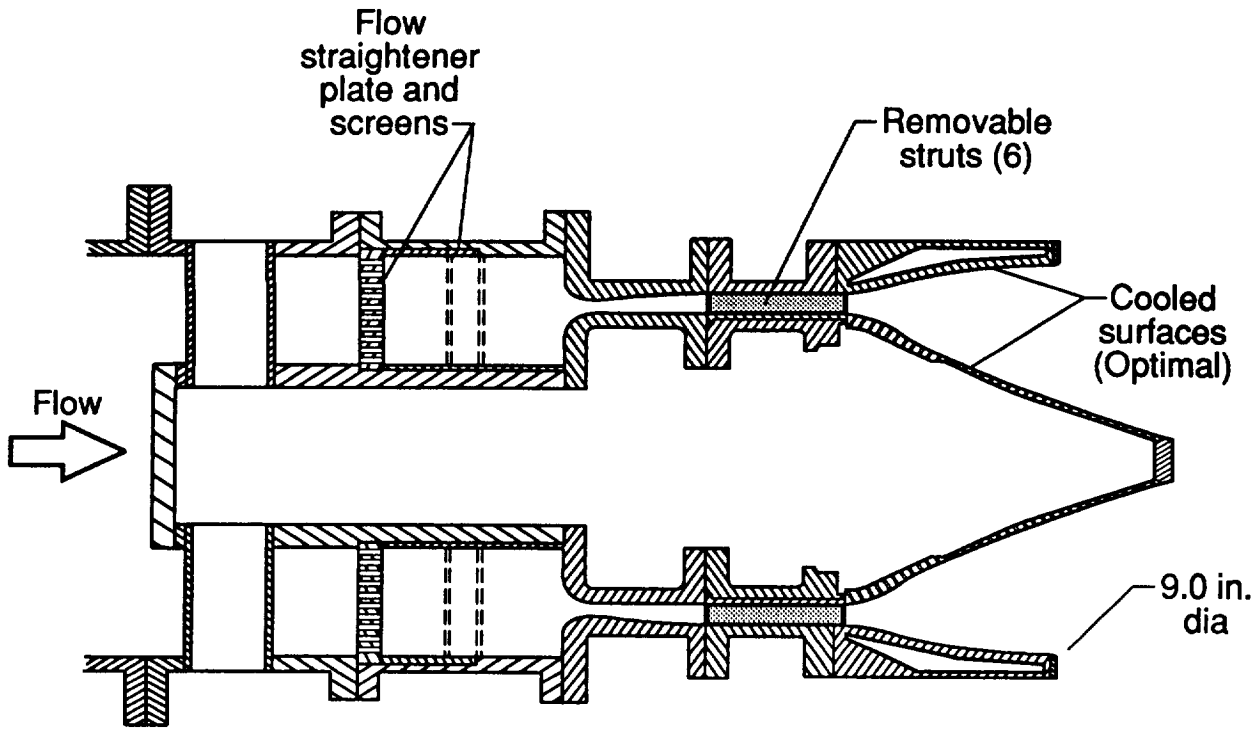
EA051993.1c

c) Effect of fuel burning upon pressure distributions; 2-D true-scale combustor, first-stage fuel injectors.

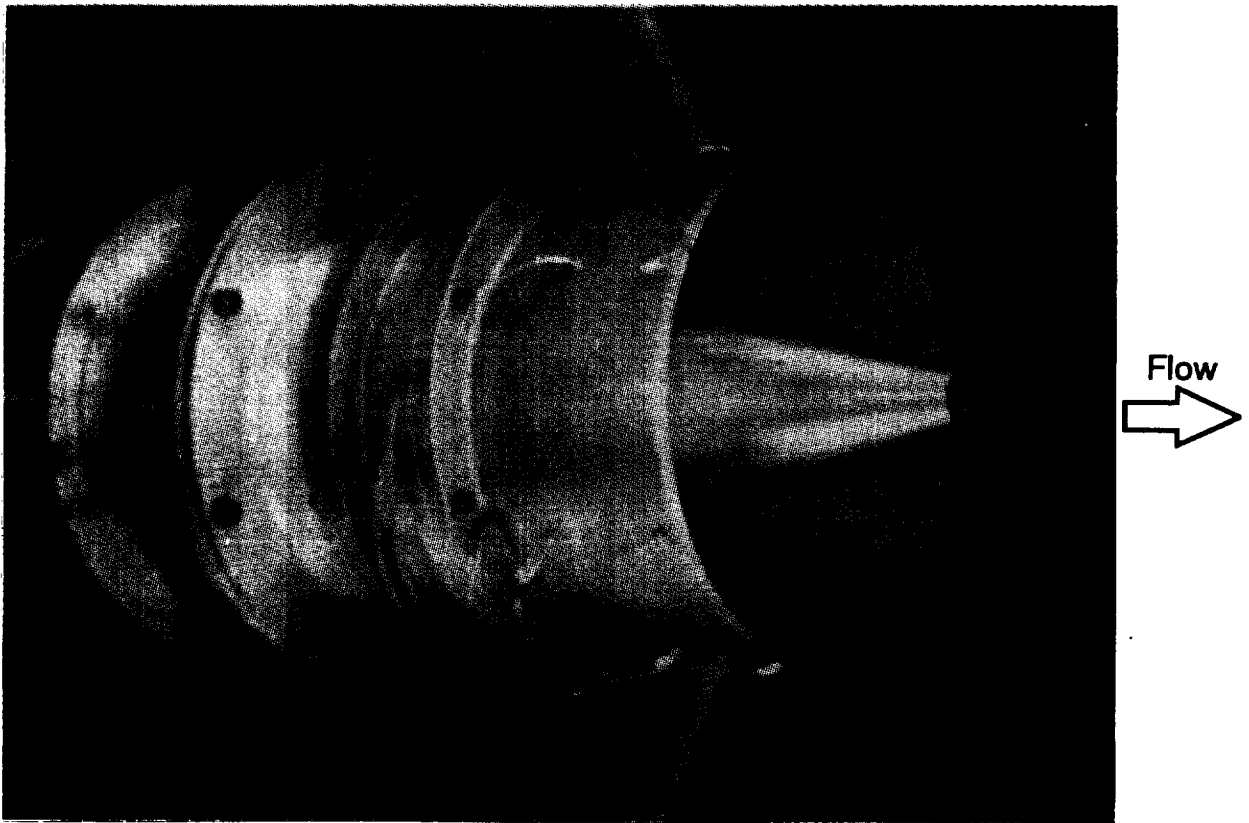


EA051993.1d

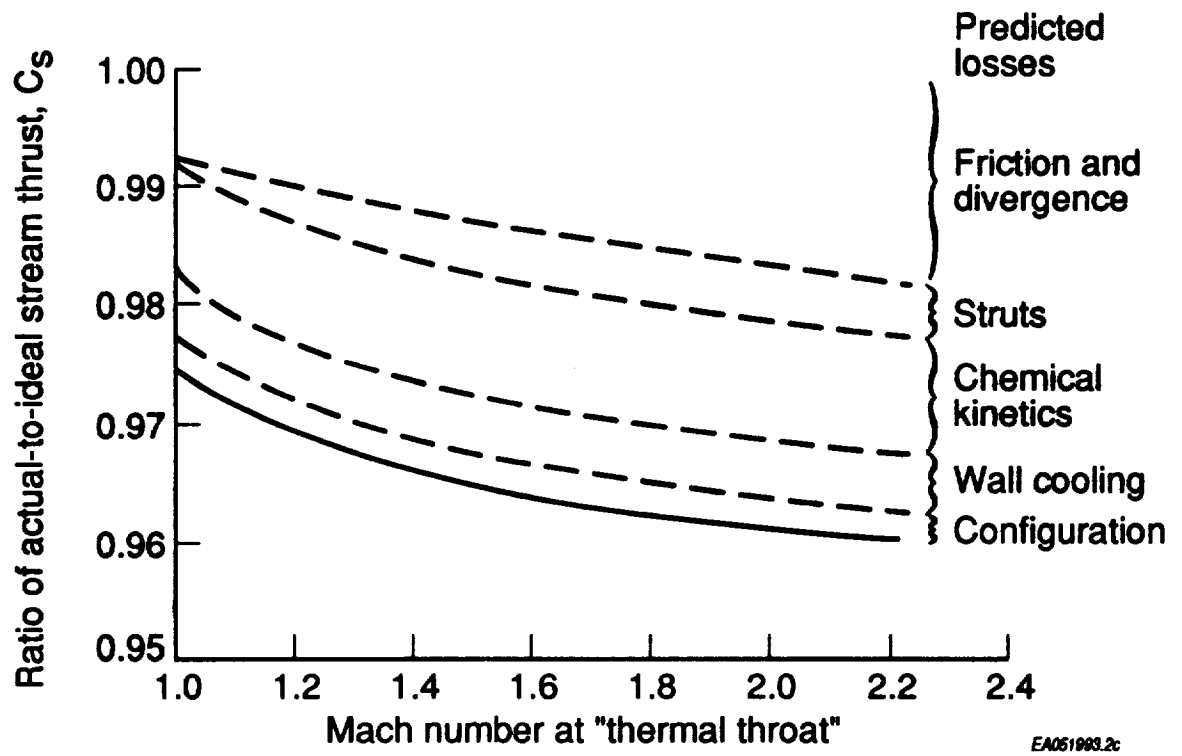
d) Combustor model scale effect; 2-D combustor, first-stage fuel injectors.



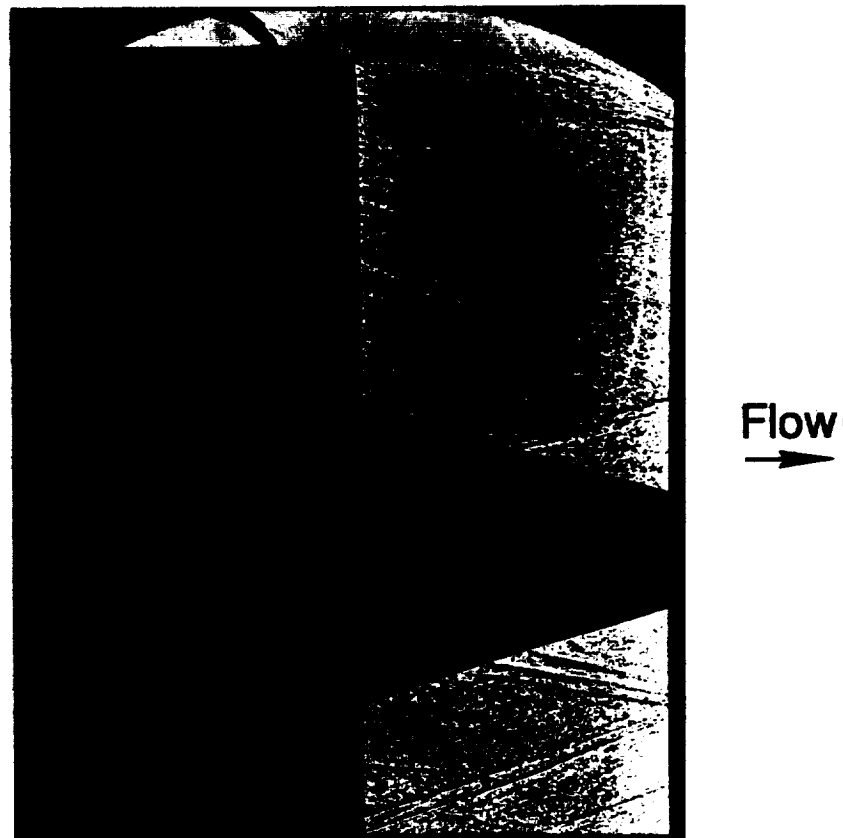
a) Model schematic.



b) Model installed in Fluidyne nozzle test facility.



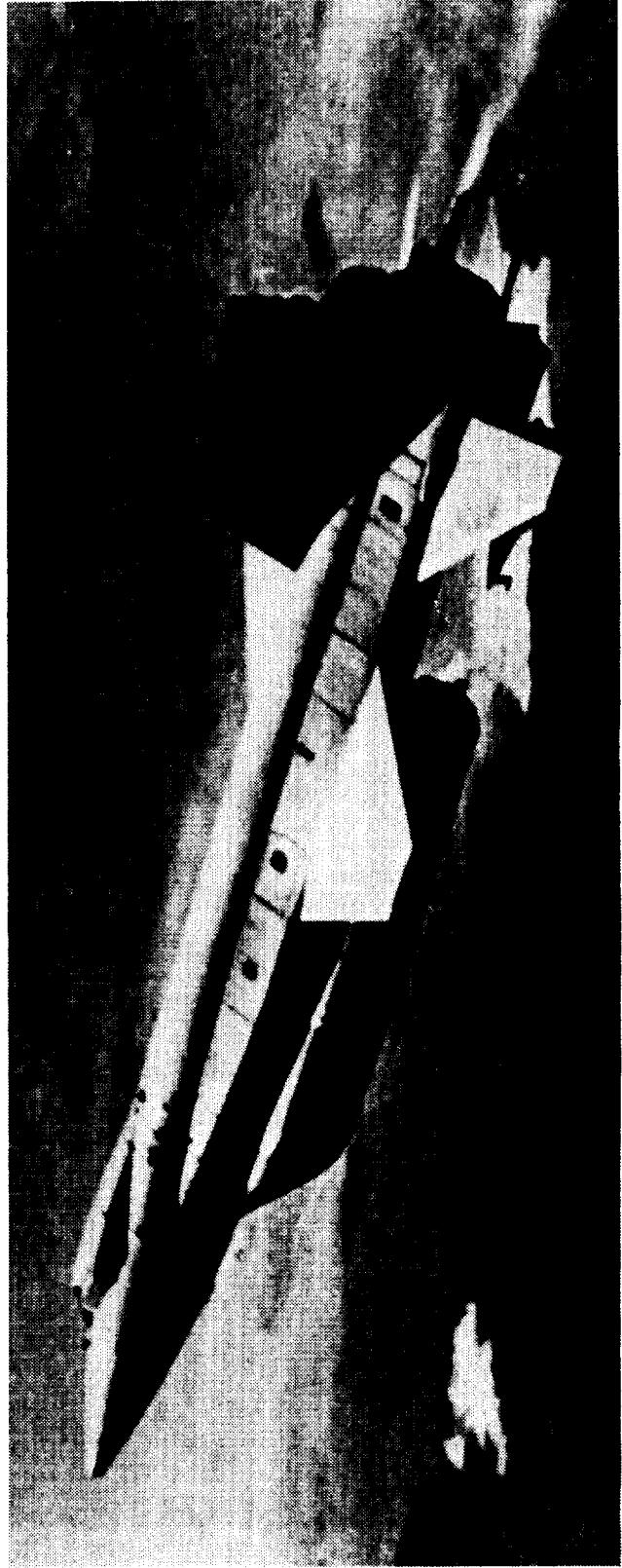
c) Estimated nozzle performances.



d) Shadowgraph of nozzle test.

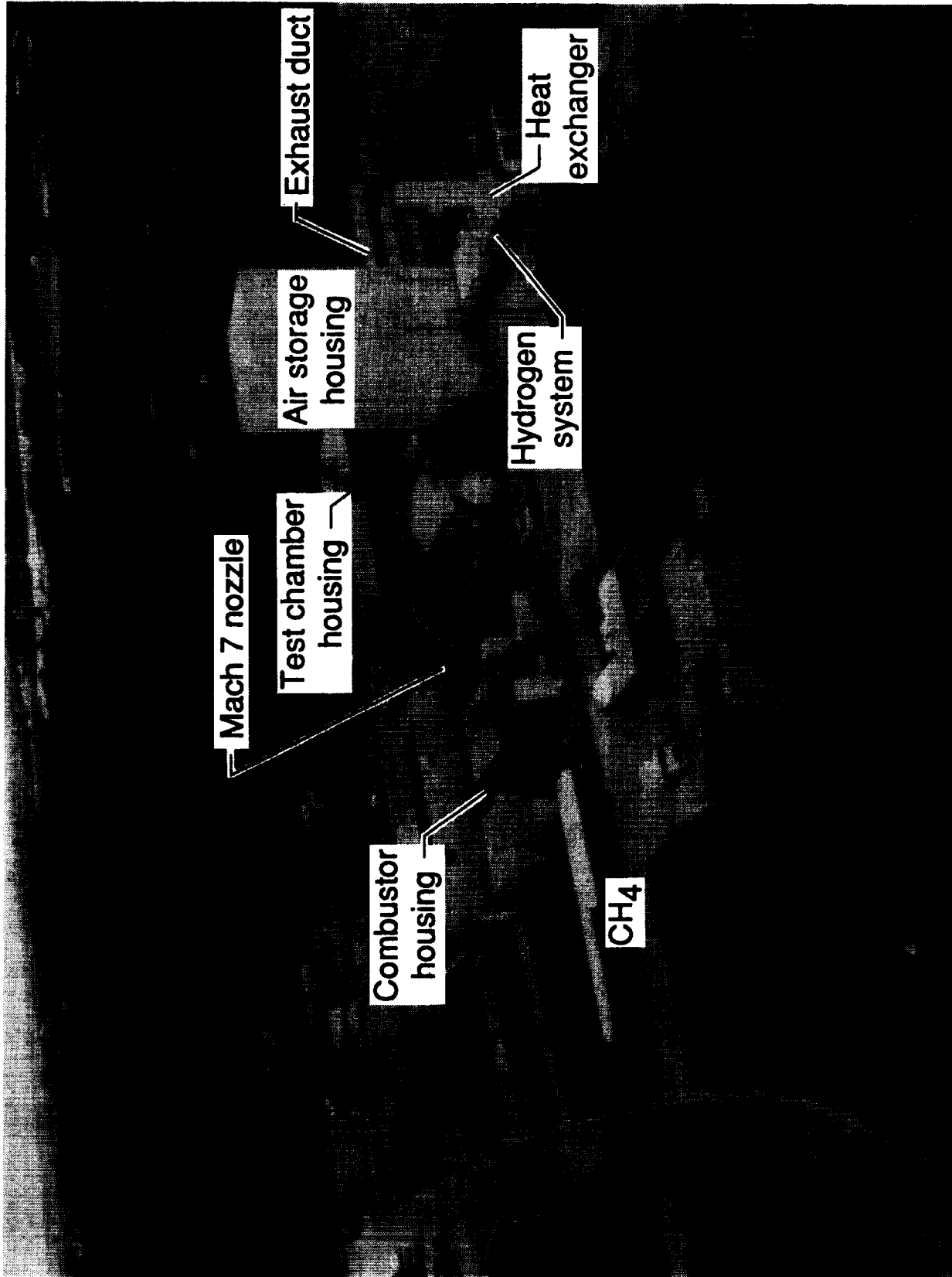


a) Mach 3.5 flight.



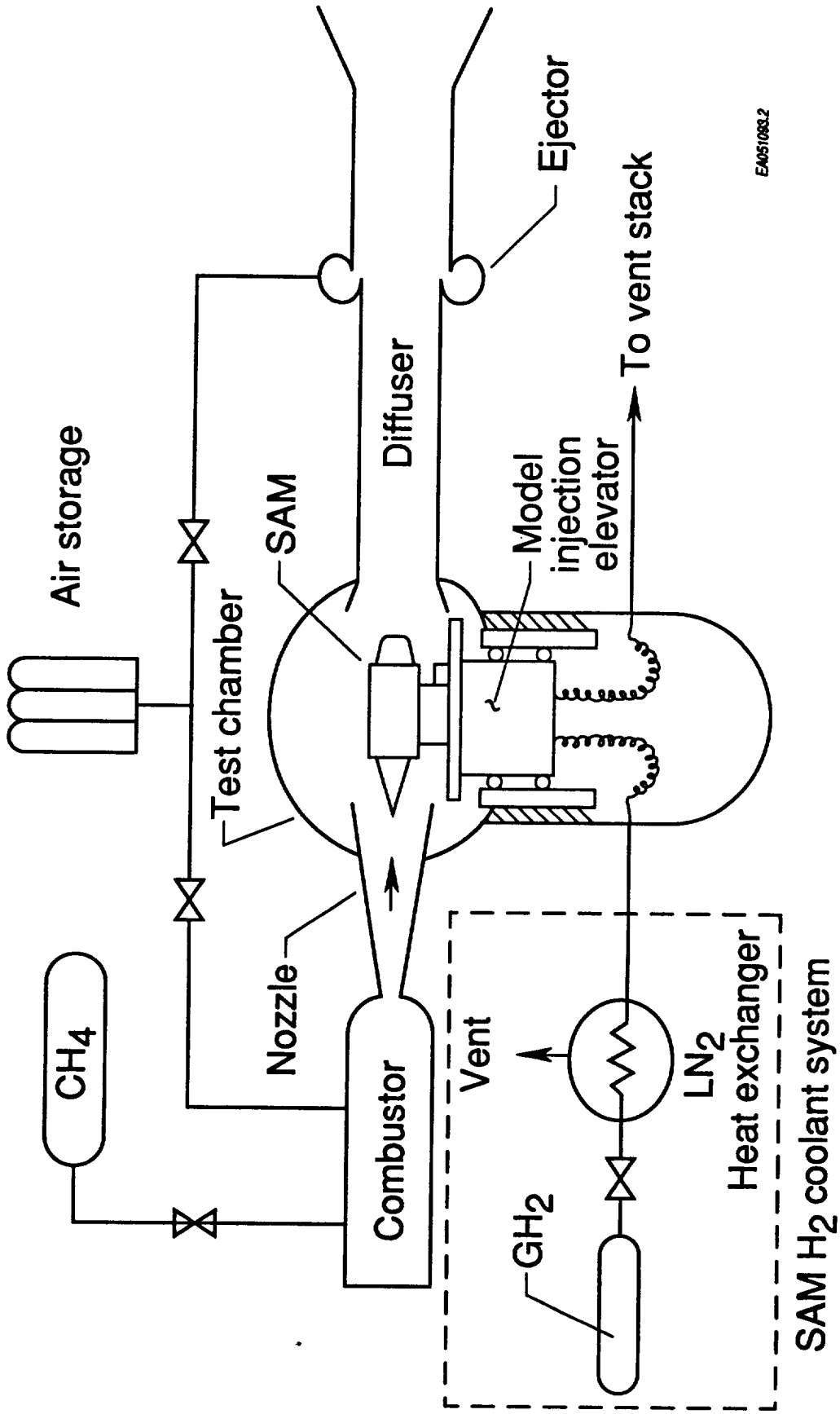
b) Mach 6.7 flight.

Figure 7.- X-15A-2 aircraft flights with simulated HRE attached.



a) Aerial photograph.

Figure 8.- NASA Langley 8-Foot High-Temperature Structures Tunnel.



EA051083.2

b) Facility schematic.

Figure 8.- Concluded.

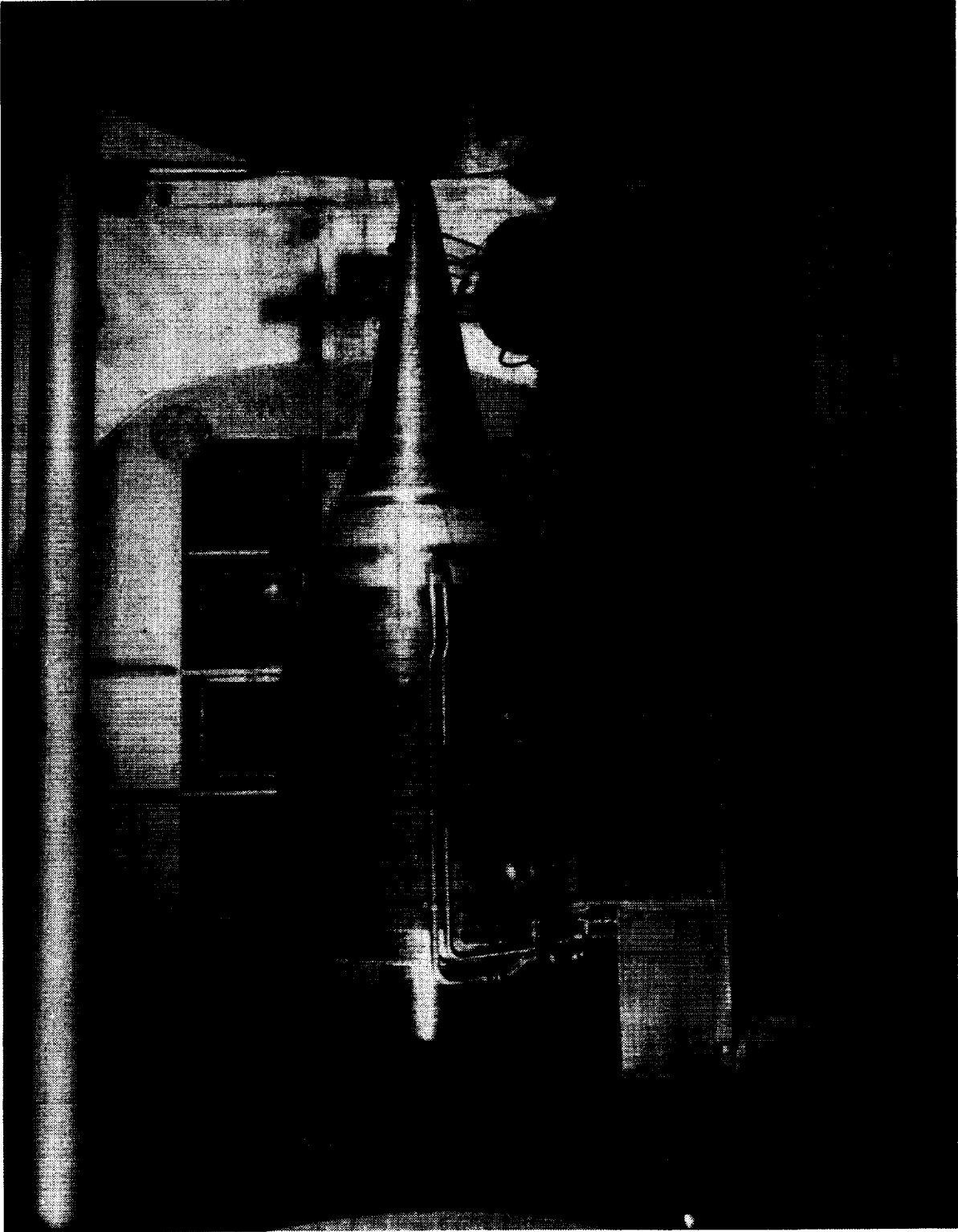
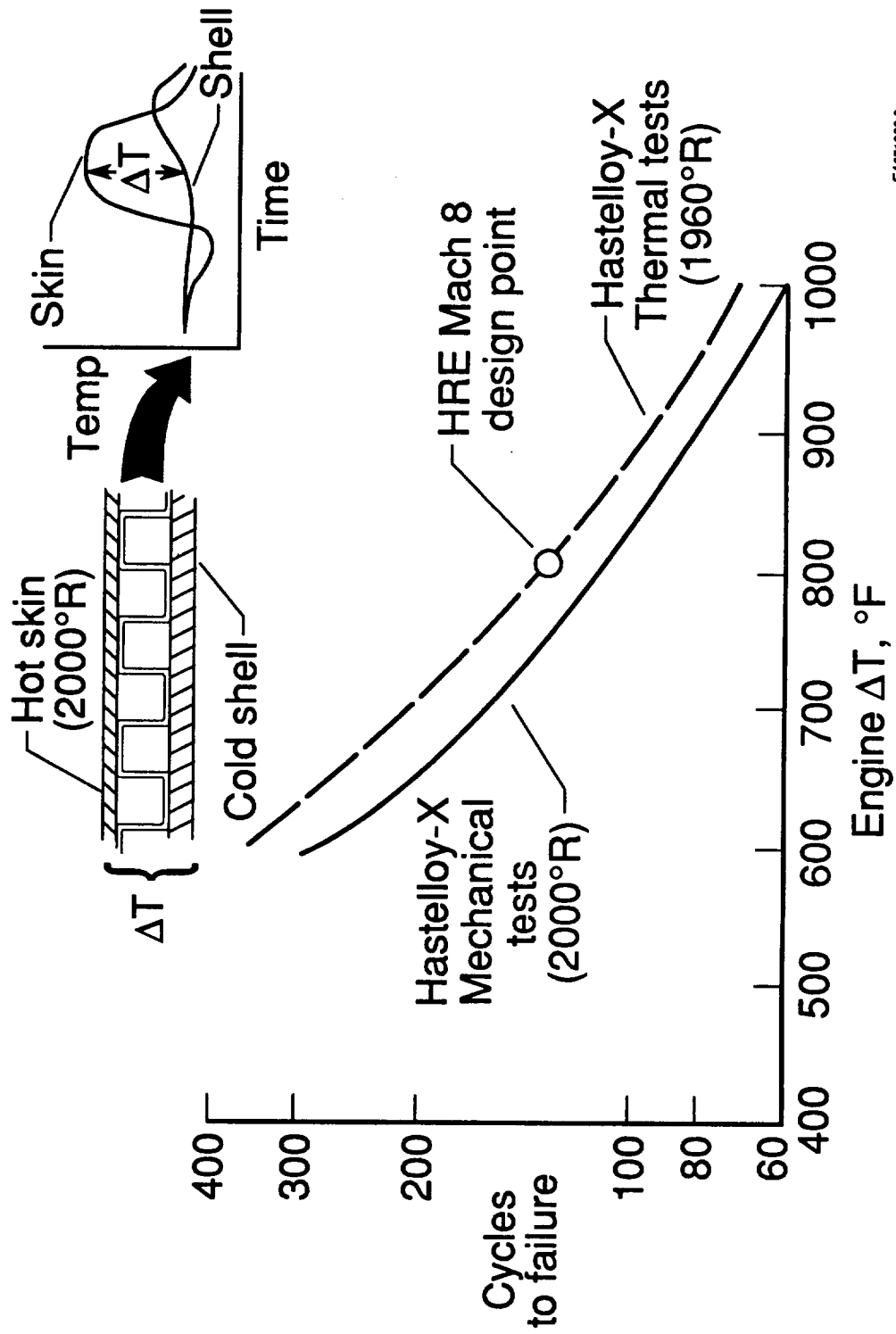
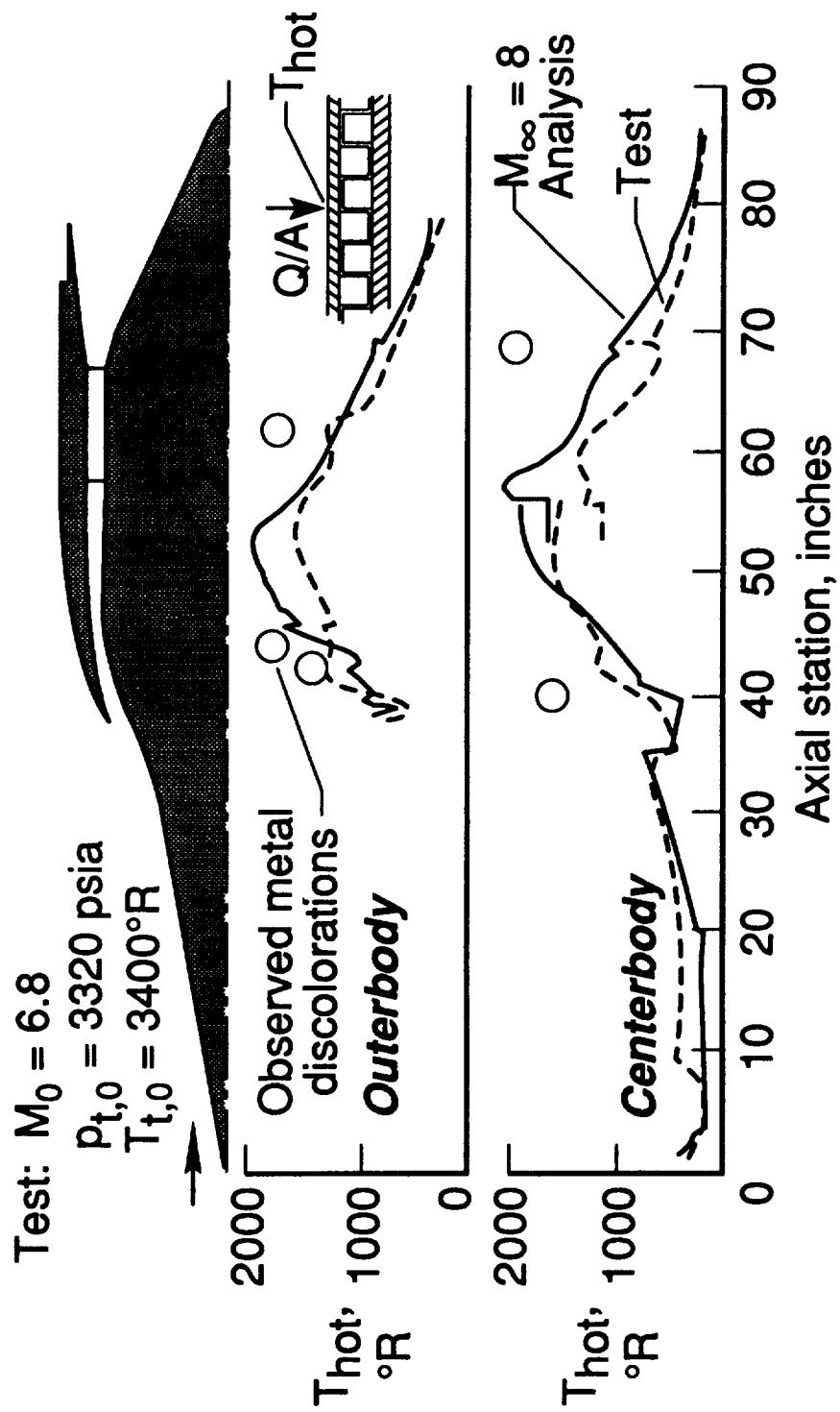


Figure 9. - SAM installed in the NASA Langley 8-Foot High-Temperature Structures Tunnel.



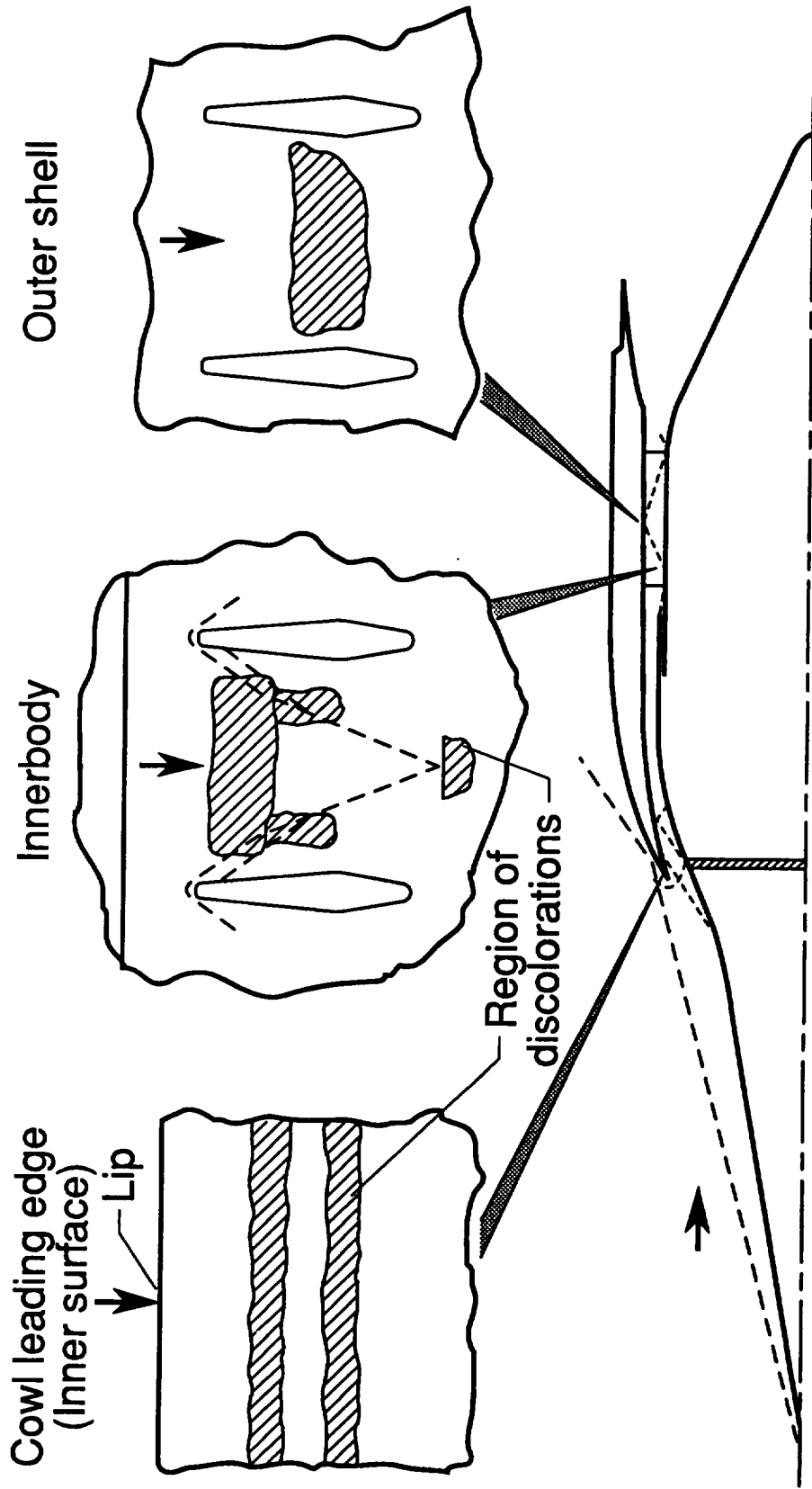
EA051083.3

Figure 10.- Low cycle fatigue test results; Hastelloy-X.



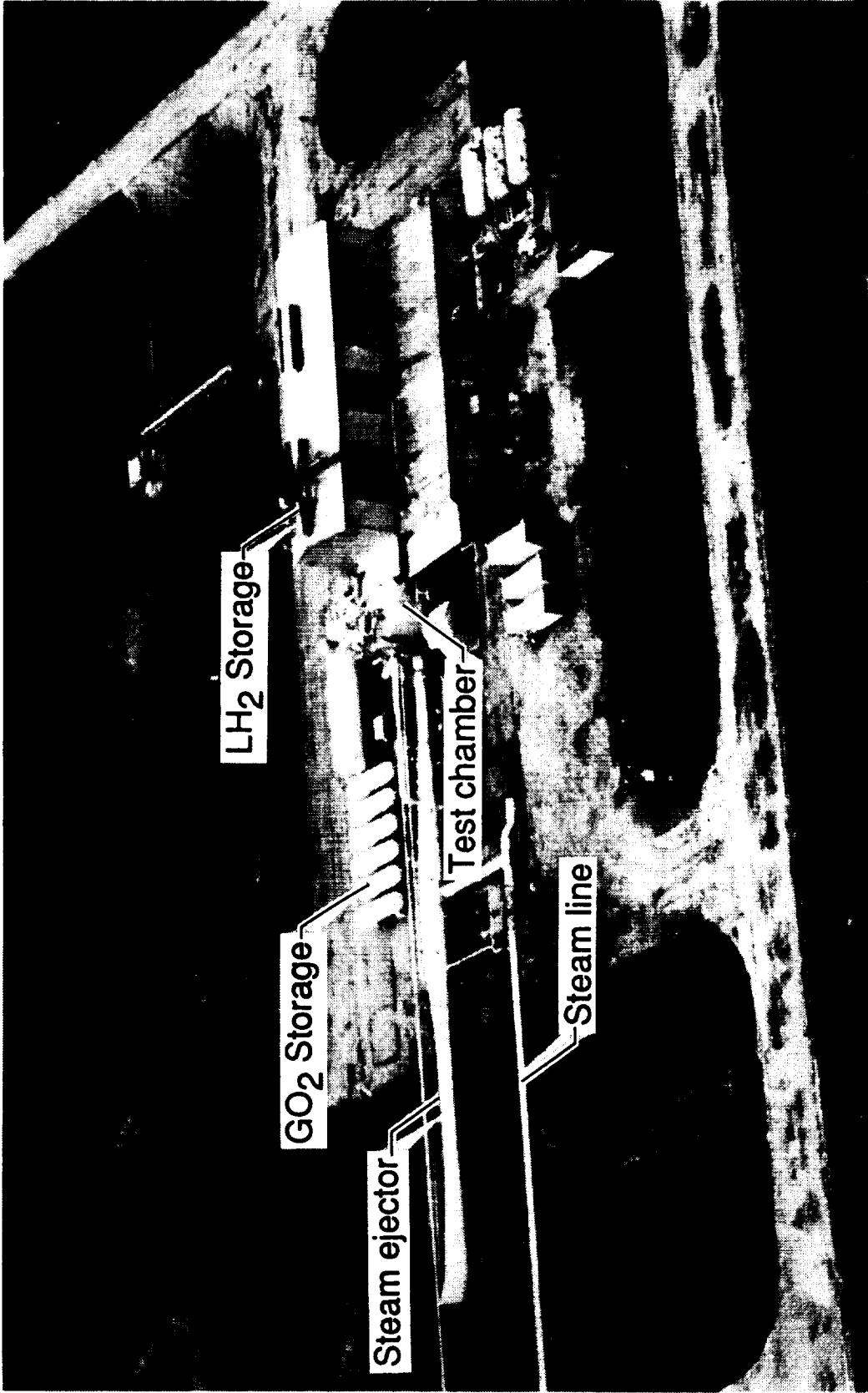
EA040786.5A00A

Figure 11.- SAM surface temperatures.

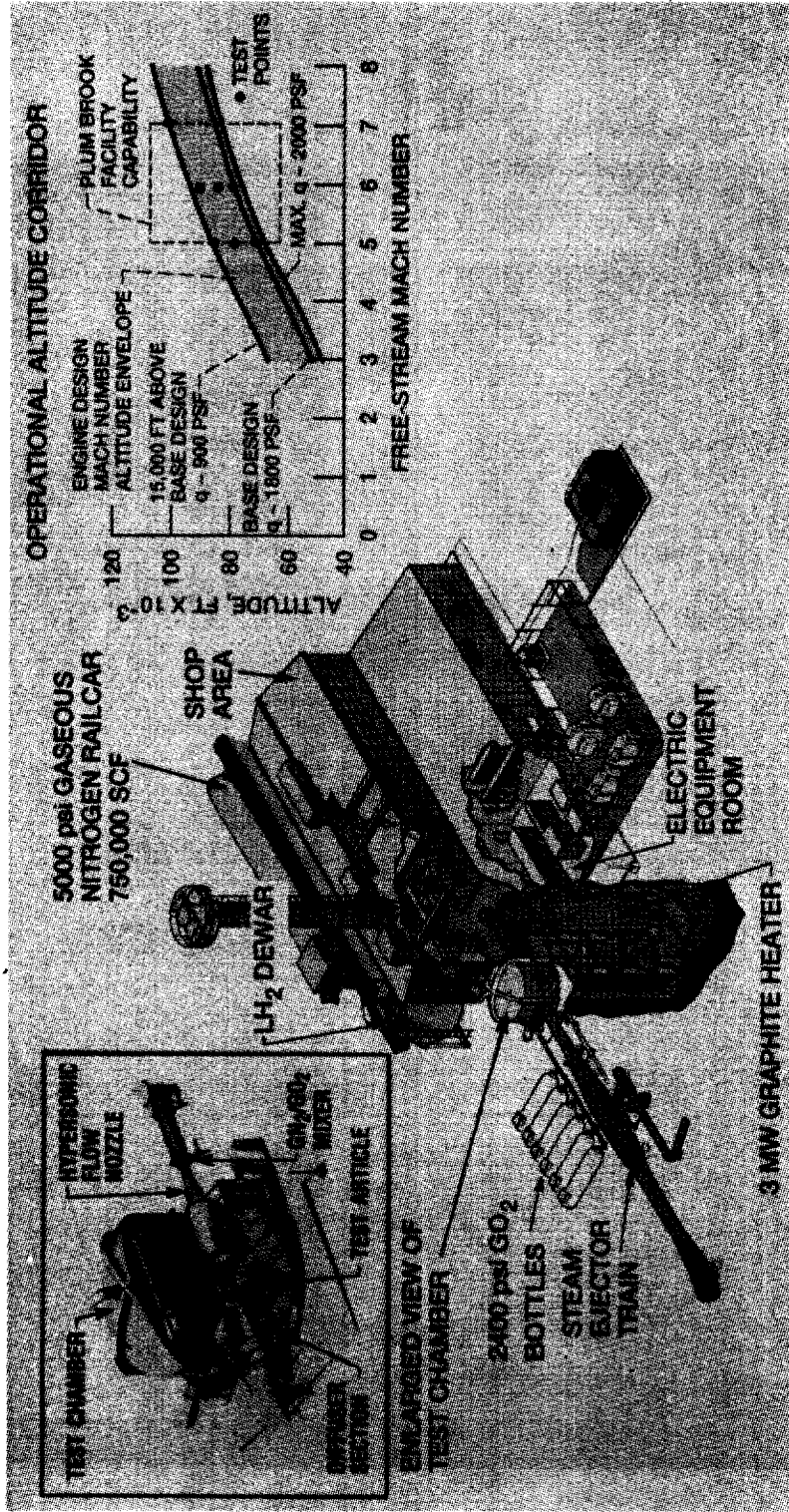


EAS1083.5

Figure 12.- SAM regions of metal surface discolorations due to high temperatures created by shock impingement.



a) Aerial photograph.
Figure 13. - NASA Lewis Plum Brook Hypersonic Tunnel Facility.



b) Cutaway view with inserts of test chamber and facility capability; artist's concept.

Figure 13.- Concluded.

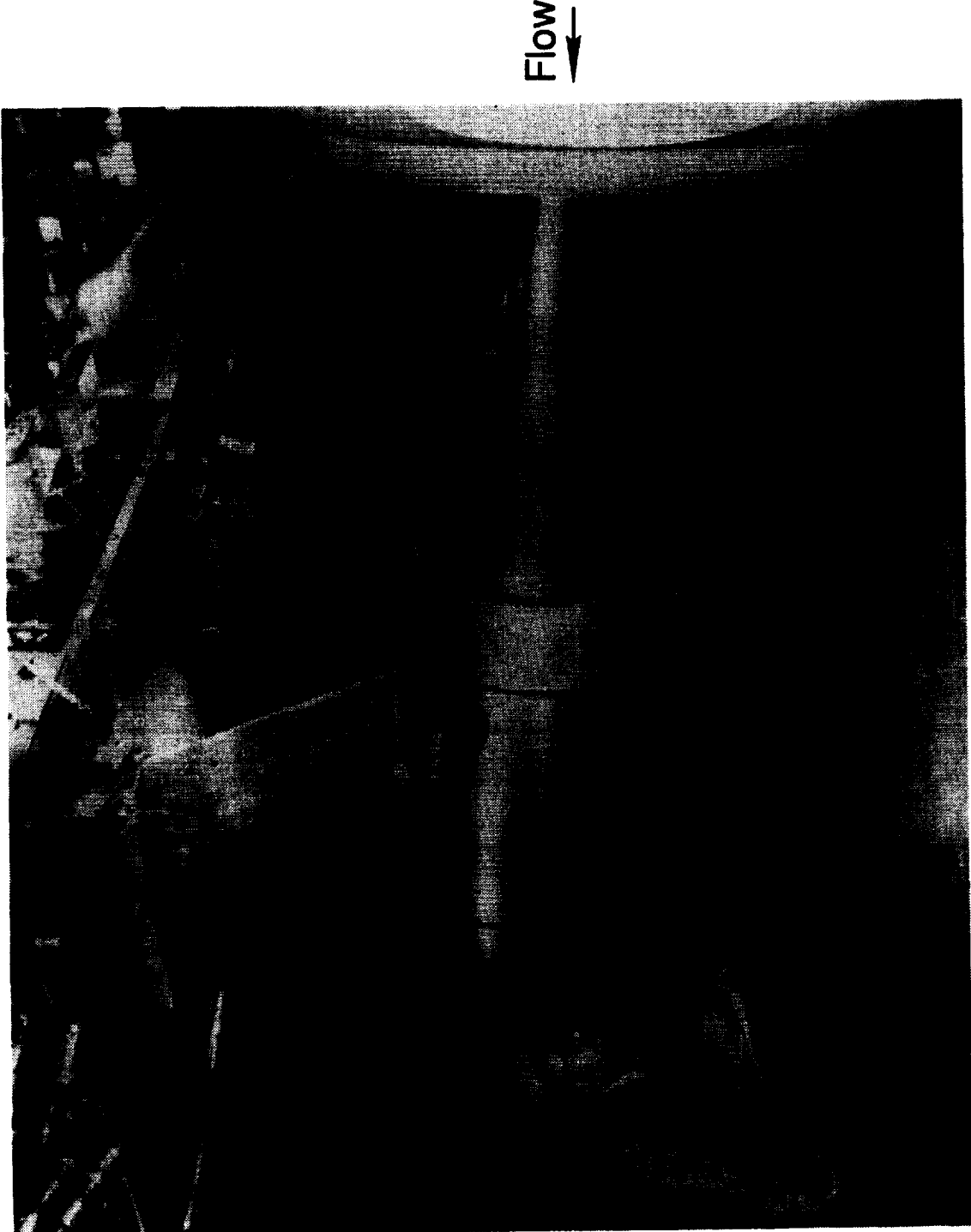


Figure 14.- AIM installed in the NASA Lewis Plum Brook Hypersonic Tunnel Facility.

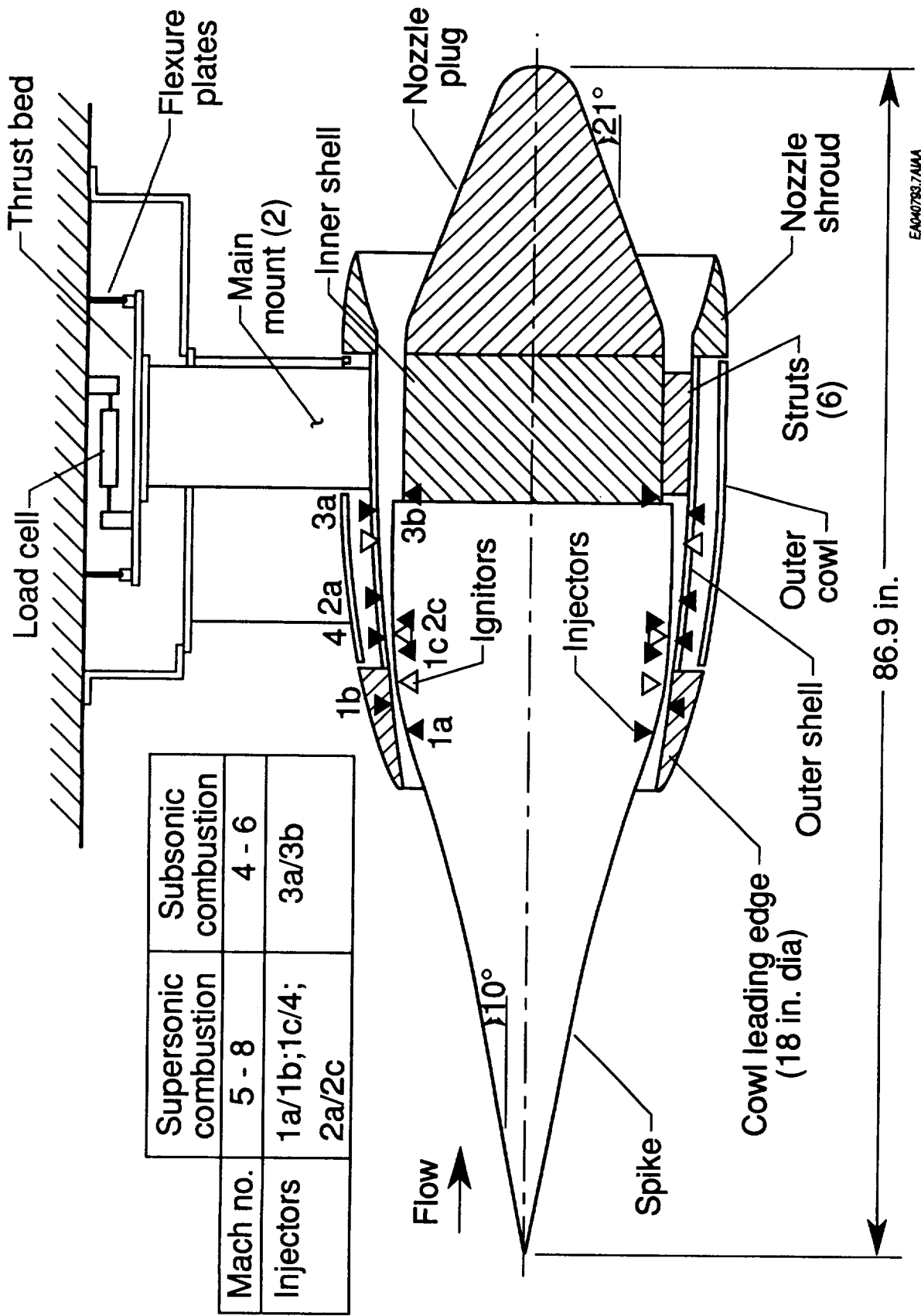


Figure 15. - AIM design features and installation schematic; boiler-plate fabrication with water cooling and gaseous hydrogen fuel.

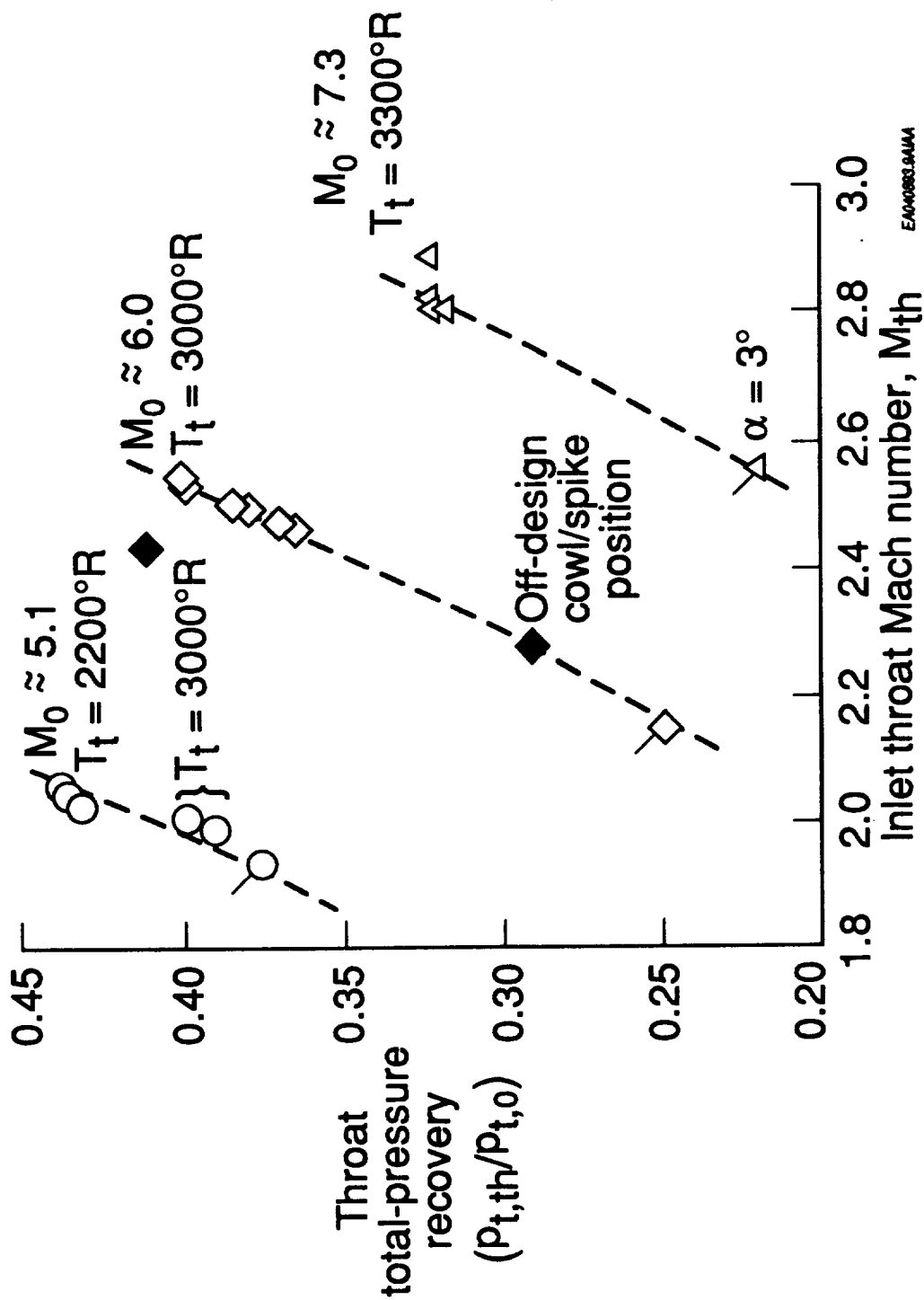


Figure 16.- AIM inlet performance; supersonic total-pressure recovery. EAO40883.0A1A

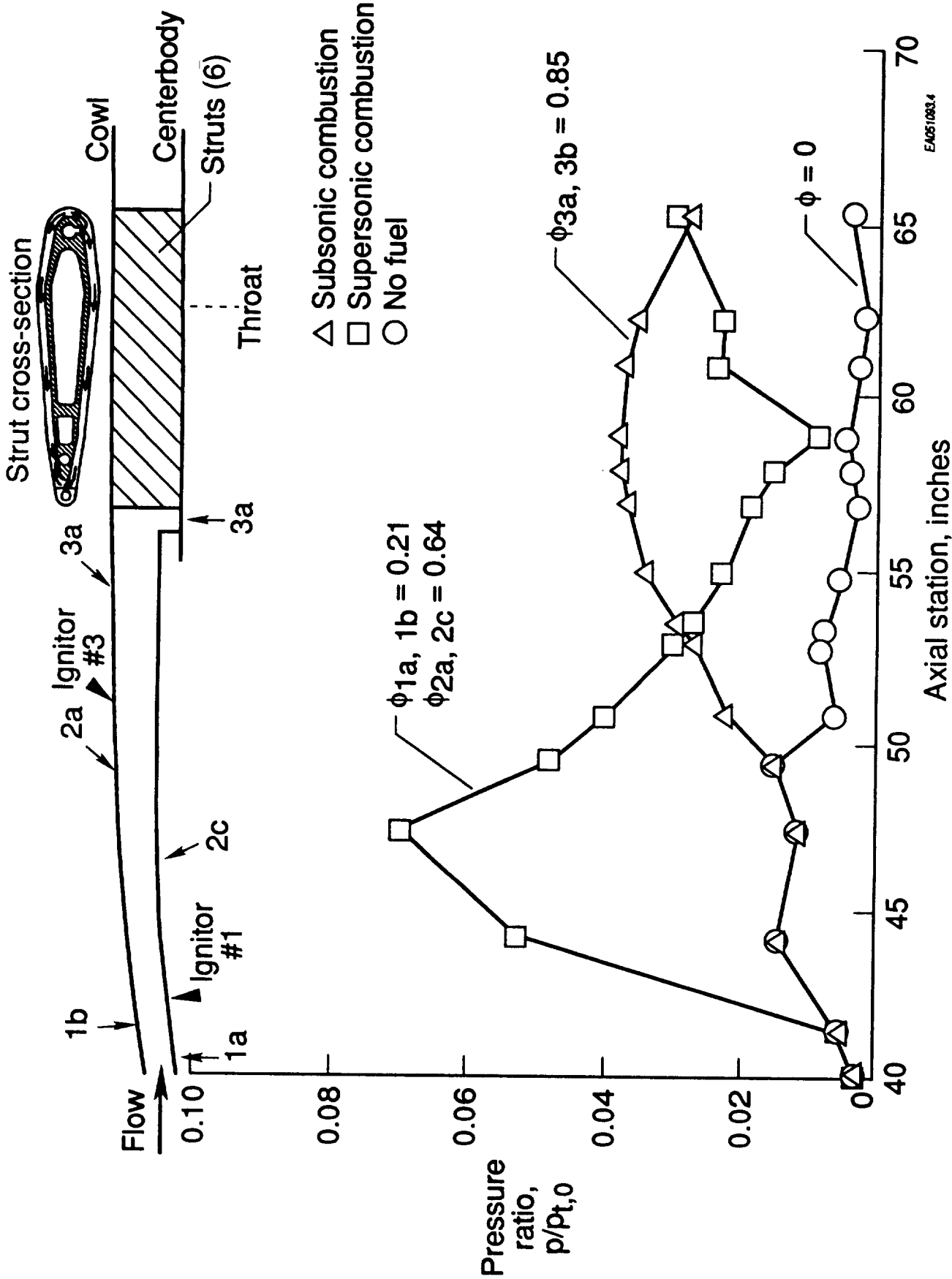
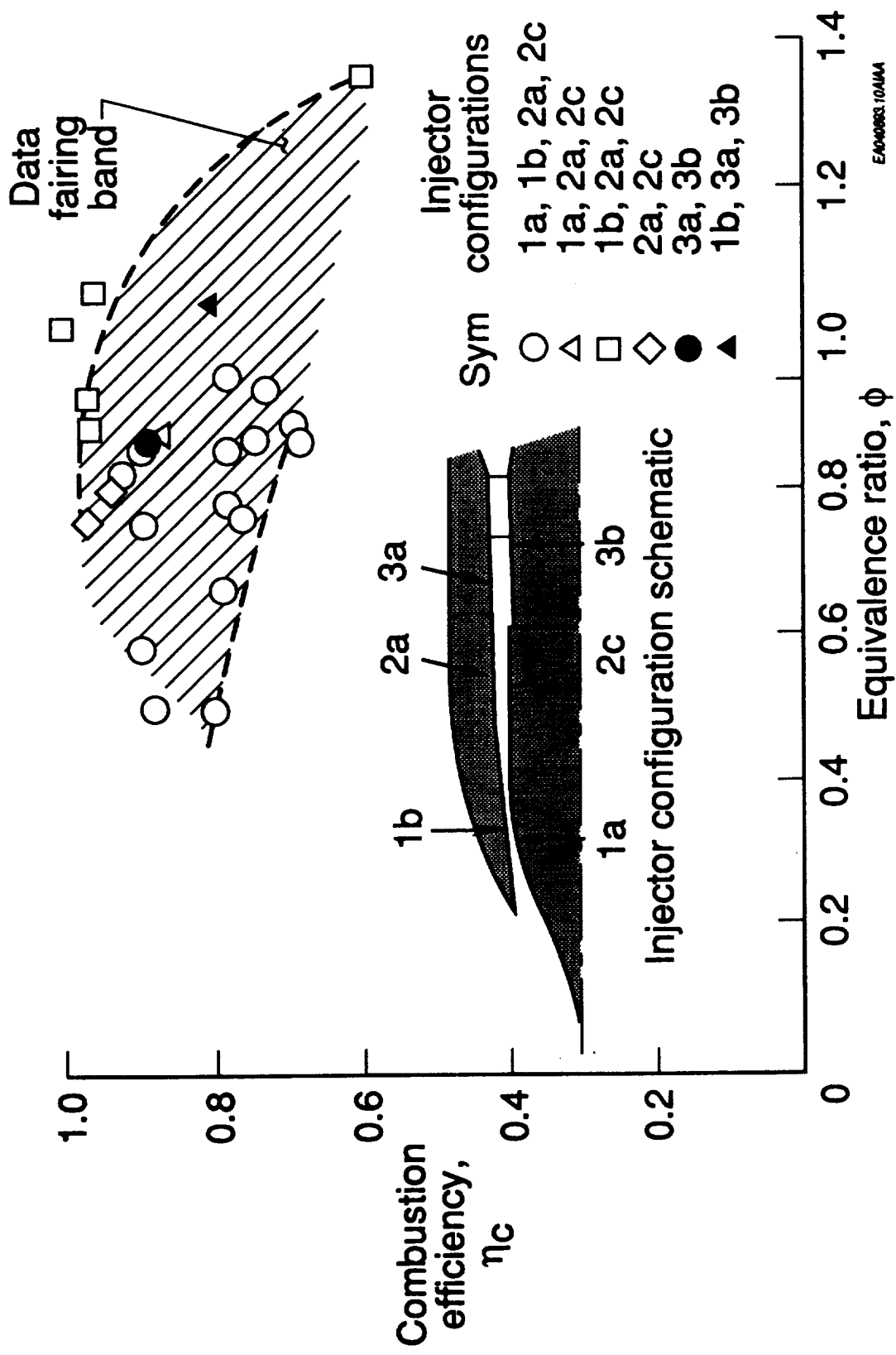
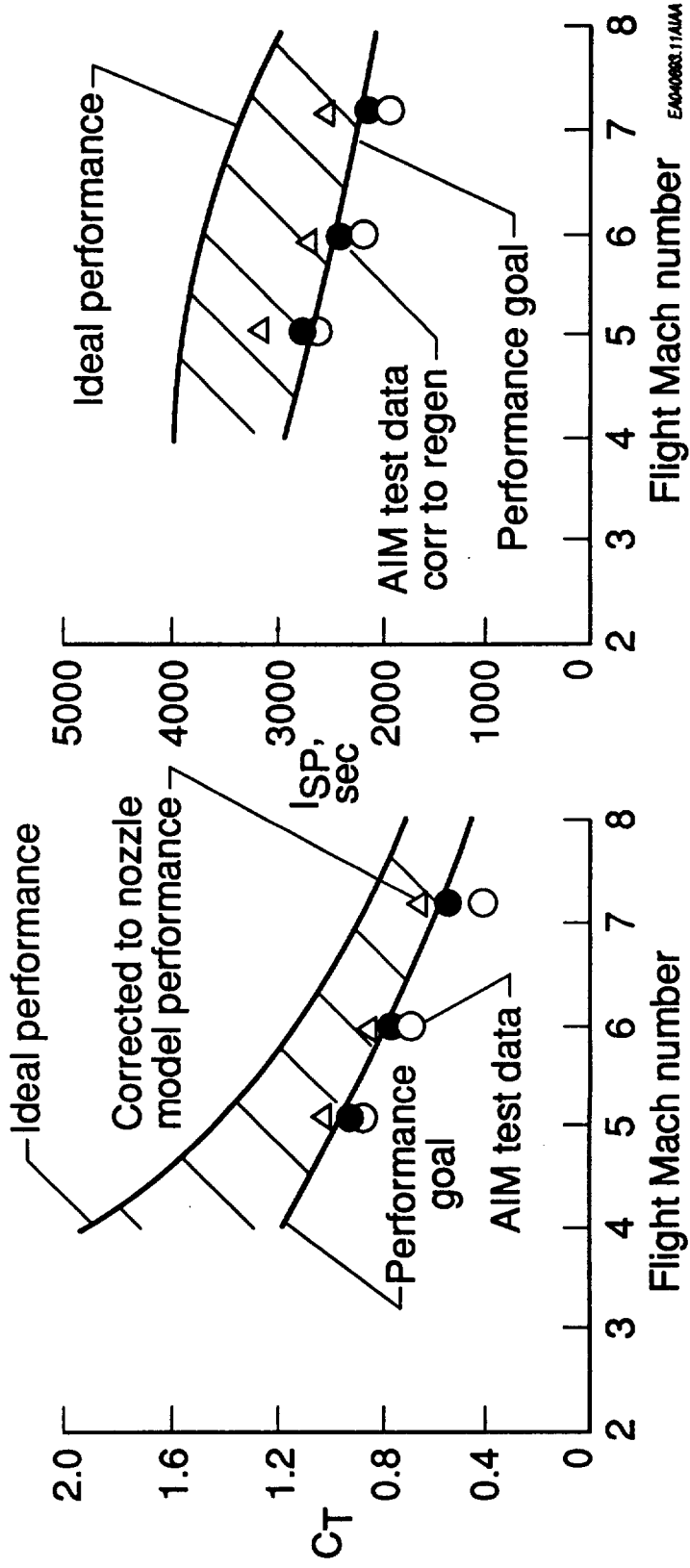


Figure 17.- AIM combustor surface pressure distributions; cowl inner surface, Mach 6.0 tests, supersonic and subsonic combustion.



E/A000083 10/11/11

Figure 18.- AIM combustor performance; Mach 6 tests.



a) Thrust coefficient, C_T .

b) Specific impulse, ISP.

Figure 19.- AIM internal performance; $\phi = 1.0$.

E4040883.11/AAA

REPORT DOCUMENTATION PAGE			Form Approved OMB No. 0704-0188	
Public reporting burden for this collection of information is estimated to average 1 hour per response, including the time for reviewing instructions, searching existing data sources, gathering and maintaining the data needed, and completing and reviewing the collection of information. Send comments regarding this burden estimate or any other aspect of this collection of information, including suggestions for reducing this burden, to Washington Headquarters Services, Directorate for Information Operations and Reports, 1215 Jefferson Davis Highway, Suite 1204, Arlington, VA 22202-4302, and to the Office of Management and Budget, Paperwork Reduction Project (0704-0188), Washington, DC 20503.				
1. AGENCY USE ONLY (Leave blank)	2. REPORT DATE October 1994	3. REPORT TYPE AND DATES COVERED Technical Memorandum		
4. TITLE AND SUBTITLE NASA's Hypersonic Research Engine Project - A Review			5. FUNDING NUMBERS 505-70-62-03	
6. AUTHOR(S) Earl H. Andrews and Ernest A. Mackley				
7. PERFORMING ORGANIZATION NAME(S) AND ADDRESS(ES) NASA Langley Research Center Hampton, VA 23681-0001			8. PERFORMING ORGANIZATION REPORT NUMBER	
9. SPONSORING / MONITORING AGENCY NAME(S) AND ADDRESS(ES) National Aeronautics and Space Administration Washington, DC 20546-0001			10. SPONSORING / MONITORING AGENCY REPORT NUMBER NASA TM-107759	
11. SUPPLEMENTARY NOTES Expanded version with an extensive list of HRE documentation (Appendix) of AIAA Paper 93-2323 presented at the AIAA 29th Joint Propulsion Conference and Exhibit, Monterey, California, June 28-30, 1993.				
12a. DISTRIBUTION / AVAILABILITY STATEMENT Unclassified - Unlimited Subject Category 07			12b. DISTRIBUTION CODE	
13. ABSTRACT (Maximum 200 words) The goals of the NASA Hypersonic Research Engine (HRE) Project, which began in 1964, were to design, develop, and construct a high-performance hypersonic research ramjet/scramjet engine for flight tests of the developed concept over the speed range of Mach 4 to 8. The project was planned to be accomplished in three phases: project definition, research engine development, and flight test using the X-15A-2 research airplane, which was modified to carry hydrogen fuel for the research engine. The project goal of an engine flight test was eliminated when the X-15 program was canceled in 1968. Ground tests of full-scale engine models then became the focus of the project. Two axisymmetric full-scale engine models, having 18-inch-diameter cowls, were fabricated and tested: a structural model and a combustion/propulsion model. A brief historical review of the project, with salient features, typical data results, and lessons learned, is presented. An extensive number of documents were generated during the HRE Project and are listed.				
14. SUBJECT TERMS HRE; ramjet/scramjet; airbreathing propulsion; wind tunnel testing; X-15/HRE flight tests			15. NUMBER OF PAGES 56	
			16. PRICE CODE A04	
17. SECURITY CLASSIFICATION OF REPORT Unclassified	18. SECURITY CLASSIFICATION OF THIS PAGE Unclassified	19. SECURITY CLASSIFICATION OF ABSTRACT Unclassified	20. LIMITATION OF ABSTRACT	